HAZEL YÜCEL

Ph.D. Thesis

2018

AN INVERSE SOURCE PROBLEM CONNECTED THERMOACOUSTIC IMAGING IN MULTI-LAYER PLANAR MEDIUM

HAZEL YÜCEL

IŞIK UNIVERSITY
2018

AN INVERSE SOURCE PROBLEM CONNECTED THERMOACOUSTIC IMAGING IN MULTI-LAYER PLANAR MEDIUM

HAZEL YÜCEL
B.S., Anadolu University, Mathematics, 2009
M.S., Anadolu University, Mathematics, 2012
Ph.D., Işık University, Mathematics, 2018

Submitted to the Graduate School of Science and Engineering
in partial fulfillment of the requirements for the degree of
Doctor of Philosophy Program
In
Mathematics

IŞIK UNIVERSITY
2018

IŞIK UNIVERSITY
GRADUATE SCHOOL OF SCIENCE AND ENGINEERING

AN INVERSE SOURCE PROBLEM CONNECTED THERMOACOUSTIC IMAGING IN MULTI-LAYER PLANAR MEDIUM

HAZEL YÜCEL

APPROVED BY:

Prof. Dr. Banu UZUN (Thesis Supervisor)	Işık University
Prof. Dr. Nalan ANTAR	İstanbul Teknik University
Assoc. Prof. Dr. Sinan ÖZEREN	İstanbul Teknik University
Assoc. Prof. Dr. Serkan SÜTLÜ	Işık University
Assoc. Prof. Dr. Özgür ÖZDEMİR	İstanbul Teknik University

APPROVAL DATE: 04/06/2018

AN INVERSE SOURCE PROBLEM CONNECTED THERMOACOUSTIC IMAGING IN MULTI-LAYER PLANAR MEDIUM

Abstract

In this thesis, we mentioned imaging technics used today, and microwave induced thermoacoustic procedure and imaging. We made literature survey about solution of the thermoacoustic equation for homogeneous and inhomogeneous medium. We modelled the inhomogenity of medium as a multi-layer planar structure and defined initial condition, continuity conditions on the layer boundaries and radiation conditions at infinity, then we derived analytical forward and inverse solution of the thermoacoustic wave equation for inhomogeneous medium with the source distribution existing in all layers. Our solution of inverse source problem is based on the methods of the Green's functions for layered planar media. For qualitative testing and comparison of the point-spread functions associated with the conventional solution for homogeneous medium and our derived layered solutions, we performed numerical simulations. In numerical simulations first we generated the measured data by using the derived forward solution for multi-layer planar medium and then we used conventional inverse solution and our derived inverse solution to image source distribution. Our simulation results showed that the conventional inverse solution based on homogeneous medium assumption, as expected, produced incorrect locations of point sources, whereas our inverse solution involving the multi-layer planar medium produced point sources at the correct source locations. Also, we showed that the performance of layered inverse solution is sensitive to the validity of the layer parameters and medium parameters used as prior information in the measured data. Our inverse solutions based on multi-layer planar media are applicable for cross-sectional 2 dimensional imaging of the organs such as breast, skin, and abdominal structure.

Keywords: Inverse source problem, thermoacoustic imaging, Green's functions.

DÜZLEMSEL ÇOK KATMANLI ORTAMDA TERMOAKUSTİK GÖRÜNTÜLEMEYLE BAĞLANTILI TERS KAYNAK PROBLEMİ

Özet

Bu tezde, günümüzde kullanılan görüntüleme tekniklerinden ve mikrodalga kaynaklı termoakustik prosedür ve görüntüleme yöntemlerininden bahsettik. Homojen ve homojen olmayan ortam için termoakustik denklemin çözümü hakkında literatür taraması yaptık. Ortamın homojen olmayışını çok katmanlı düzlemsel bir yapı olarak modelledik. Başlangıç koşulu, katman sınırında süreklilik koşulu ve sonsuzda radyasyon koşulları altında, termoakustik dalga denkleminin homojen olmayan ortam ve kaynak dağılımının her yerde olduğu varsayımıyla, analitik olarak ileri ve ters çözümlerini elde ettik. Katmanlı düzlemsel olarak modellenmiş yapı için ters kaynak probleminin çözümünde Green fonksiyonlar yöntemi kullandık. Literatürdeki homojen ortam için elde edilen çözüm ve katmanlı ortam için elde ettiğimiz çözümü karşılaştırdık ve nitel testler için kaynak fonksiyonu olarak nokta yayılım fonksiyonunu kullanarak sayısal benzetimler yaptık. Sayısal benzetimde ilk olarak katmanlı ortam için elde ettiğimiz ileri çözümü kullanarak ölçülen data ürettik ve daha sonra bu ürettiğimiz ölçülen datayı literatürde var olan ve bizim elde ettiğimiz ters çözümde kullanarak, ortamdaki kaynak dağılımını görüntüledik. Sayısal benzetimler sonucunda, çok katmanlı düzlemsel ortam için elde ettiğimiz ters çözümün noktasal kaynak yerlerini tam olarak doğru gösterdiğini, fakat literatürde var olan homojen ortam varsayımına dayanan ters çözümün beklendiği gibi noktasal kaynak yerlerini yanlış gösterdiğini gösterdik. Ayrıca bilgisayar benzetimlerini kullanarak, katmanlı ortam için elde ettiğimiz ters çözümün performansının ve görüntü kalitesinin, önceki bilgiler olarak kullanılan katman parametrelerinin ve ortam parametrelerinin doğruluğuna duyarlı olduğunu ve bu parametrelerin termoakustik görüntüleme kalitesini etkilediğini gösterdik. Çok katmanlı düzlemsel ortam için elde ettiğimiz ters çözüm meme, deri ve karın bölgesi gibi organların 2 boyutlu kesitsel görüntülenmesi için uygulanabilir.

Anahtar kelimeler: Ters kaynak problemi, termoakustik görüntüleme, Green fonksiyonları.

Acknowledgements

I would like to express my gratitude towards to my advisor Prof. Dr. Banu Uzun for guidance and continuous support throughout my studies.

I would like to express my sincere gratitude to my coadvisor Prof. Dr. Mustafa Karaman who had a serious illness and then deceased in January 2018, for motivation, immense knowledge and encouragement during my studies and researches.

Lastly, I would like to thank my family for supporting me throughout all my life.

This work was supported by TUBITAK of Turkey through ARDEB-1003 Program under Grant 213E038.

To my son.

Table of Contents

List of Figures

List of Abbreviations

$\mathbf{P}$	Fourier Transform Of Acoustic Wave Function In Time Domain
$\mathbf{G}$	Fourier Transform Of Green's Function In Time Domain
ω	Angular Frequency
k_x	Spatial Frequency In The x Direction
k_y	Spatial Frequency In The y Direction
k_z	Spatial Frequency In The z Direction
ω	Angular Frequency
k	Wave Number

Chapter 1

Introduction

Thermoacoustic imaging is a hybrid biomedical imaging modality, combining the high contrast, the good tissue penetration of microwave, and the high spatial resolution of ultrasound imaging without harmful side effects. This technique is an up-to-date issue that has not yet become a clinical tool with scientific, technological and commercial potential. Thermoacoustic imaging is quite useful especially in breast cancer diagnosis and following, imaging of skin and abdominal structure.

Today, X-Ray Computed Tomography, Magnetic Resonance Imaging and Ultrasound are most widely used medical imaging [1]. X-Rays is very cost-effective technique but it has cancer-triggering harmful side effect. In contrast magnetic resonans imaging gives good results at diagnosis of malign cancer, but this imaging technique is relatively expensive and has no standart application protocoles. Ultrasonic imaging is low-cost and has no harmful side-effects [2]. Point resolution of ultrasonic imaging is high, but contrast resolution is poor; this complicates the early diagnosis of some cancers and distinguishing the tumour if it is benign and malign.

In thermoacoustic wave generation, the tissue is irradiated by pulsed microwave excitation and the microwave energy is selectively absorbed by different tissue structures with different dielectric parameters. It is converted to heat pulse which

causes generation of acoustic waves by thermoelastic expansion and then the thermoacoustic signals are detected by the ultrasound transducers to be used for the image reconstruction of the mediums. Thermoacoustic tomography combines the high contrast and good tissue penetration of microwave and high spatial resolution of ultrasound imaging without harmful side effects [3–9]. Only nonionizing wave is used in this techniques and the relationships between thermoacoustic signals and the physical parameters of biological tissues are well defined and these properties makes them ideal in vivo applications.

This thesis is organized as follows. In Chapter 2, we mention the literature about microwave-induced thermoacoustic imaging. In Chapter 3, we give some the necessary information for derivation of the solution of the thermoacoustic problem. In Chapter 4, we introduce briefly the medical imaging modalities. In Chapter 5, we touch on the principles of microwave - induced thermoacoustic imaging and identify our problem with boundary conditions, and derive the forward and inverse solution of thermoacoustic equation involving multi-layer planar medium with source distribution existing in all layers. In Chapter 6, we calculate the coefficients of the Green's function for homogeneous and two-layer medium in two dimensional Cartesian coordinates. In Chapter 7, we present numerical simulation for qualitative testing and comparison of the point-spread functions associated with the literature-homogeneous and our derived layered solutions using the coefficients obtained in Chapter 6. In chapter 8, we mention the difference between the our derived inverse solution and the solution in literature and discuss the advantage of the our derived inverse solution. Also, we explain in what areas the solution we have proven can be used.

Chapter 2

Literature Survey

Thermoacoustic tomography is studied by several research groups to increase the image quality and image depth at the international level [10–12]. Kruger et al. [13] developed instrumentation for measuring the tissue absorption properties of radio waves in human body using thermoacoustic interactions. Additionally, the basic principles of thermoacoustic imaging and different implementations along with a reference list are given in [14, 16–18, 20].

Xu and Wang [21,22] solved the inverse problem for homogeneous medium bounded by two parallel planes, an infinitely long circular cylinder and a sphere. They used expansions involving exponential, Bessel and Legendre functions, respectively. Idemen and Alkumru [23] gave an exact formula for the inverse source problem assuming that reflection of the pressure on the boundary of the biological medium is negligibly small and medium is homogeneous. Schoonover and Anastasio [24] have presented a solution of thermoacoutsic wave equation involving layered media with the source is assumed to be confined to only one-known layer. In addition to acoustically homogeneous situations, the acoustic inverse initial value problem with heterogeneous speed of sound studied for thermoacoustic and photoacoustic tomography [25–29]. Idemen presented some universal properties of the Green's functions associated with the wave equation in bounded partially-homogeneous domains [30].

Chapter 3

Preliminary Information

3.1 Fourier Transform

3.1.1 Time Fourier Transformation

In our reconstruction, the Time - Fourier transform of $f(t) \in L^1(-\infty, \infty)$ is

$$F(\omega) = \int_{-\infty}^{\infty} f(t) e^{i\omega t} dt, \quad \omega \in (-\infty, \infty) \tag{3.1}$$

and, inversely

$$f(t) = \frac{1}{2\pi} \int_{-\infty}^{\infty} f(\omega) e^{-i\omega t} d\omega, \quad t \in (-\infty, \infty). \tag{3.2}$$

3.1.2 Spatial Fourier Transform (2 - Dimensional)

In our reconstruction, Spatial - Fourier transform of $f(x, y, z) \in L^1(-\infty, \infty)$ is

$$\hat{f}(k_x, k_y, z) = \iint_{-\infty}^{\infty} f(x, y, z) exp(-i(k_x x + k_y y)) dx dy, \quad k_x, k_y \in (-\infty, \infty) \tag{3.3}$$

and, inversely

$$f(x, y, z) = \frac{1}{(2\pi)^2} \iint_{-\infty}^{\infty} \hat{f}(k_x, k_y, z) exp(i(k_x x + k_y y)) dk_x dk_y, \quad x, y \in (-\infty, \infty). \tag{3.4}$$

3.2 Dirac Delta Function

Dirac delta function is a generalized function, or distribution that is introduced for modelling the density of an idealized point mass or point charge.

Properties:

a) This function is equal to $0 \in \mathbb{R}$ everywhere except 0.

b) Integral over the entire real line of Dirac delta function is equal to one.

c) Fourier transform of Dirac delta function is

$$F(\delta(t)) = 1, \quad t \in (-\infty, \infty). \tag{3.5}$$

d) Fourier transform of the time derivative of Dirac delta function is

$$F(\delta(t)') = -i\omega, \quad \omega \in (-\infty, \infty). \tag{3.6}$$

e) For any $\epsilon > 0$ and any function $f(\mathbf{r})$ that is continuous over $(\mathbf{r_0} - \epsilon, \mathbf{r_0} + \epsilon)$, we have

$$\int_{\mathbf{r_0}-\epsilon}^{\mathbf{r_0}+\epsilon} f(\mathbf{r})\delta(\mathbf{r} - \mathbf{r_0})d\mathbf{r} = \int_{-\infty}^{\infty} f(\mathbf{r})\delta(\mathbf{r} - \mathbf{r_0})d\mathbf{r} = f(\mathbf{r_0}). \tag{3.7}$$

3.3 Kronecker Delta Function

The Kronecker delta δ_{ij} is defined as a function of two arguments i and j. If i and j are the same (i.e. $i = j$) then the function δ_{ij} is equal to 1. Otherwise (i.e. $i \neq j$) the Kronecker delta is equal to 0. Formally, this is written as

$$\delta_{ij} = \begin{cases} 1 & i = j \\ 0 & i \neq j \end{cases}. \tag{3.8}$$

3.4 Divergence Theorem

Let D be a solid in $\mathbb{R}^3$, bounded by a piecewise smooth surface S. Let $F(x, y, z)$ $= P(x, y, z)i + Q(x, y, z)j + R(x, y, z)k$ be a vector field such that P, Q and R are continuous and have continuous first order partial derivatives in an open set containing D. Assume $\mathbf{n}$ is the unit outward normal to the surface S. Then

$$\iint_S (\mathbf{F}.\mathbf{n})ds = \iiint_V (\text{div}\mathbf{F})dV. \tag{3.9}$$

3.5 Derivation Of The Thermoacoustic Equation

Before we derive the thermoacoustic equation, we derive the acoustic wave equation.

3.5.1 Derivation Of Acoustic Wave Equation

Here, a longitudinal small-amplitude acoustic plane wave propagation in a homogeneous medium in the x direction is considered. We explore the motion of a differential volume element $dV = dxdydz$ at position x:
a) The material equation with the excess pressure p is a function of the mass density ρ :

$$p = p(\rho). \tag{3.10}$$

We can expand this equation to the first order of the Taylor series around the equilibrium mass density ρ_0 as follows:

$$p - p_0 = \left(\frac{\partial p}{\partial \rho}\right)(\rho - \rho_0), \tag{3.11}$$

ρ_0 denotes the equilibrium pressure. The condensation at any point is defined as

$$s = \frac{\rho - \rho_0}{\rho_0}, \tag{3.12}$$

that is

$$\rho = \rho_0(1 + s). \tag{3.13}$$

Since the acoustic wave has a small amplitude, the essential restriction condensation must be small, $\mid s \mid \ll 1$. Substituting (3.13) into (3.11), we obtain

$$p - p_0 = \rho_0 \left(\frac{\partial p}{\partial \rho}\right) s. \tag{3.14}$$

b) We derive the force equation. In the absence of viscosity, the net force F on the element experienced by the differential volume element in x direction is given by

$$F = -\left(\frac{\partial p}{\partial x}\right) dxdydz. \tag{3.15}$$

Using Newton's second law, we have

$$-\frac{\partial p}{\partial x} = \rho_0 \frac{\partial u}{\partial t}, \tag{3.16}$$

where u is the medium velocity and t is the time respectively. Since $\mid s \mid \ll 1$, we replace the ρ by ρ_0 by using (3.13) and yield

$$-\frac{\partial p}{\partial x} = \rho_0 \frac{\partial u}{\partial t}. \tag{3.17}$$

This equation is called linear inviscid force equation, which can be generalized to $3D$ space as $-\nabla = \rho_0(\frac{\partial \vec{u}}{\partial t})$. If we substitute (3.14) into (3.17), we obtain

$$-\frac{\partial s}{\partial x} = \frac{1}{\partial p/\partial \rho} \frac{\partial u}{\partial t}. \tag{3.18}$$

c) We derive the force equation based on the conservation of mass as follows:

$$-\frac{\partial p}{\partial t} = \frac{\partial(\rho u)}{\partial x}, \tag{3.19}$$

and this equation can be generalized to $-(\frac{\partial p}{\partial t}) = \nabla.(\rho\vec{u})$. We expand the right hand side of (3.19) as

$$\frac{\partial(\rho u)}{\partial x} = \rho\frac{\partial u}{\partial x} + \frac{\partial \rho}{\partial x}u. \tag{3.20}$$

Because of $\mid s \mid \ll 1$, we rewrite the above equation as follows:

$$\frac{\partial(\rho u)}{\partial x} = \rho\frac{\partial u}{\partial x} + \frac{\partial \rho}{\partial x}u. \tag{3.21}$$

Second term in (3.21) is negligible because of the subsonic medium velocity of a small amplitude wave. So, (3.19) becomes

$$-\frac{\partial \rho}{\partial t} = \rho_0\frac{\partial u}{\partial x}. \tag{3.22}$$

If we substitute (3.13) into (3.22), we obtain

$$-\frac{\partial s}{\partial t} = \frac{\partial u}{\partial x}. \tag{3.23}$$

d) Finally, differentiating (3.18) with respect to x, differentiating (3.23) with respect to t, and substracting side by side, we obtain

$$\frac{\partial^2 p}{\partial x^2} = \frac{1}{\partial p/\partial \rho}\frac{\partial^2 p}{\partial t^2}. \tag{3.24}$$

Thus, we have

$$\frac{\partial^2 p}{\partial x^2} = \frac{1}{c^2}\frac{\partial^2 p}{\partial t^2} \tag{3.25}$$

where $c^2 = \dfrac{\partial p}{\partial \rho}$ is the speed of sound in the medium. So, we can generalize to the $3D$ case as

$$\nabla^2 p = \frac{1}{c^2}\frac{\partial^2 p}{\partial t^2}. \tag{3.26}$$

It is the basic acoustic wave equation which describes the propagation of an acoustic wave in a homogeneous nondissipative medium.

3.5.2 Derivation Of The Thermoacoustic Wave Equation

Initial Thermoacoustic Pressure

On microwave or laser excitation, fractional volume expansion dV/V of the heated tissue at position $\mathbf{r}$ can be express as [31],

$$\frac{dV}{V} = -\kappa p(\mathbf{r}) + \beta T(\mathbf{r}). \tag{3.27}$$

Here, κ denotes the isothermal compressibility ($\sim 5 \times 10^{-10} Pa^{-1}$ for water or soft tissue); β denotes the thermal coefficient of the volume expansion ($\sim 4 \times 10^{-4} K^{-1}$ for muscle); p and T denote the changes in pressure (in Pascal) and temperature (in Kelvin), respectively. The isothermal compressibility κ can be expressed as

$$\kappa = \frac{C_p}{C_v \rho c^2} \tag{3.28}$$

where ρ denotes the mass density, c denotes the speed of sound, and C_p and C_v denote the specific heat capacities at constant pressure and volume, respectively.

We suppose that the microwave or laser pulse duration t_m is less than the acoustic confinement time and acoustic confinement time less than the thermal confinement time

$$t_m \ll \frac{d_c}{c} \ll \frac{d_c^2}{4\alpha_t h} \tag{3.29}$$

where d_c is the characteristic length of heat heterogeneity (the dimension of the optically absorbing target of interest or the decay constant of the optical energy deposition, whichever is smaller), and $\alpha_t h$ is the thermal diffusivity ($\sim 0.1 mm^2/s$ for tissue.) If we assume that all absorbed optical energy is converted into heat and nonthermal relaxation such as fluorescence is negligible, the temperature rise generated by the short laser pulse. And we get

$$p_0 = \frac{\beta}{\kappa c \rho C_v} A \tag{3.30}$$

where A is the specific or volumetric optical absorption (in joules per centimeter cubed, optical energy deposition density).

When the such a short laser pulse, the fractional volume expansion is negligible and the local pressure rise p_0 immediately after the laser excitation can be derived from (3.27) as

$$p_0(\mathbf{r}) = \frac{\beta T(\mathbf{r})}{\kappa}. \tag{3.31}$$

$$\Gamma = \frac{\beta}{C_v \kappa \rho} \tag{3.32}$$

is the Grueneisen parameter (dimensionless). Then, we write

$$p_0(\mathbf{r}) = \Gamma A(\mathbf{r}) \tag{3.33}$$

Thermoacoustic Equation

We write the following two equations which are responsible for thermoacoustic generation (generalized Hooke's law),

$$\nabla . \vec{u}(\mathbf{r}, t) = \kappa p(\mathbf{r}, t) + \beta T(\mathbf{r}, t) \tag{3.34}$$

and the equation of motion [32]

$$\rho \frac{\partial^2 u(\vec{\mathbf{r}}, t)}{\partial t^2} = -\nabla p(\mathbf{r}, t). \tag{3.35}$$

Here, vector $\vec{u}$ defines the medium displacement. The left hand side of (3.34) represents the fractional volume expansion, while the right hand side represents the two factors related to the volume expansion. The left hand side of (3.35) represents the mass density times the acceleration, and the right hand side represents the force applied per unit volume. If we take the divergence of (3.35), we can write

$$\rho \frac{\partial^2}{\partial t^2} [\nabla . \vec{u}(\mathbf{r}, t)] = -\nabla^2 p(\mathbf{r}, t). \tag{3.36}$$

If we substitute (3.27) into (3.36), we obtain thermoacoustic wave equation as follows:

$$\left(\nabla^2 - \frac{1}{c^2}\frac{\partial^2}{\partial t^2}\right) p(\mathbf{r}, t) = -\frac{\beta}{\kappa c^2}\frac{\partial^2 T(\mathbf{r}, t)}{\partial t^2} \tag{3.37}$$

where $c = \dfrac{1}{\sqrt{\rho\kappa}}$.

Chapter 4

Medical Imaging Modalities

4.1 X-ray Computed Tomography (CT)

X-ray computed tomography (CT) invented in 1972 and, it was the first radical change in the medical use of X- rays since Roentgen's discovery. Computed tomography uses the mathematical device of Fourier filtered back-projection. Two key progressions in diagnostic X-ray imaging followed from the introduction of the computed tomography. Firstly the CT image is a 2D reconstruction of a cross-section of the patient anatomy. Secondly, CT provides a good contrast between bone and all soft tissue. Both make the interpretation of the resulting images very much easier .

Hospitals routinely use CT for the rapid assessment of structural abnormality resulting from injury or disease throughout the body. CT has become a standard tool in the planning of the cancer radiation treatment and it provides a clear definition of the tumour and tumour's disposition with respect to the surrounding healthy tissue. However, the major risk is that the patient is exposed to large doses of radiation due to the higher doses of radiation delivered with a CT scan. With the increased radiation amounts also comes the increased risk for cancer. The CT image platform is shown in Fig. (4.1).

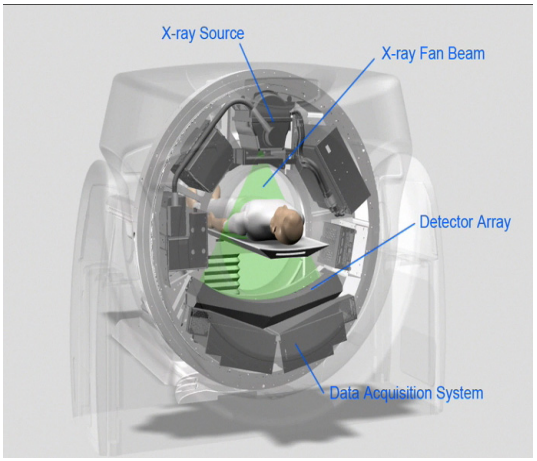

Figure 4.1: X-Ray Computed Tomography(http://www.medical-x-ray.com)

4.2 Ultrasound

Ultrasound uses sound waves to look inside a part of the body. The process can be described as follows: A gel is put on the tissue to be imaged and a hand-held instrument called a transducer is rubbed with gel and pressed against the skin. It emits sound waves and picks up the echoes as they bounce off body tissues. The echoes are converted by a computer into a black and white image on a computer screen. One is not exposed to radiation with ultrasound. Ultrasound is the only way to tell if a suspicious area is a cyst without putting a needle into it to take out fluid. Ultrasound may also be used to help doctors guide a biopsy needle into an area of concern in the tissue as the cysts cannot be accurately diagnosed by a physical examination alone. For example, breast ultrasound is used to evaluate breast problems that are found during a screening or a diagnostic mammogram, or on physical examination. It may be helpful to use ultrasound along with a mammogram when screening the women, under high cancer risk, with dense breast tissue. It is widely available, non-invasive, and less expensive than other options. Although ultrasound has the advantage of being more available and less expensive, it is less sensitive compared to Magnetic resonance imaging and CT. Also, the effectiveness of an ultrasound test depends on the operator's level of skill and experience.

4.3 Magnetic Resonance Imaging (MRI)

Magnetic resonance imaging is a tomographic technique, but without any harmful effects since it has no ionising radiation hazard. MRI generates cross-sectional images of the human body. The process is shown in Fig.(4.2). First, the process begins with positioning the imaged body in a strong, uniform magnetic field, which polarizes the nuclear magnetic moments of water protons by forcing their spins into one of two possible orientations, and second an appropriately polarized radio-frequency field, applied at resonant frequency, forces spin transitions between orientations. Then those transitions create a signal which can be detected by a receiving coil which is shown in (a), (b), (c) and (d) respectively in Fig.(4.2).

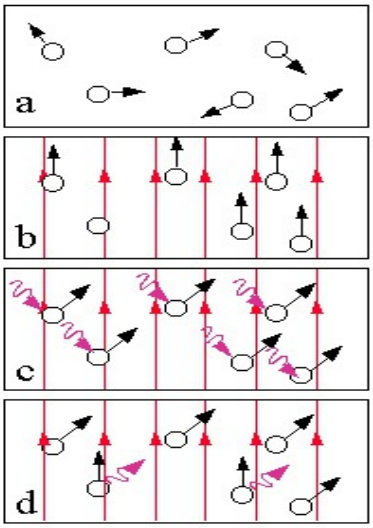

Figure 4.2: Spin Warp [http://cibsr.stanford.edu/participating/AboutMRI.html]

A MRI scanner applies the radio-frequency field as finely crafted pulses, which excite only protons whose resonant frequencies fall within a fairly narrow range. Applying magnetic-field gradients during the radio-frequency pulse creates resonant conditions for only the protons that are located in a thin, predetermined slice of the body. Orientation and thickness of this slice can be selected arbitrarily in the imaged body. These signal encodes the positional information across

the slice using a method known as the spin warp then a two-dimensional Fourier transform extracts that positional information.

MRI can be used in a person who have already been diagnosed with breast or brain cancer to determine better the actual size of the cancer, the stage of cancer and to look for any other cancers in the breast or brain. However, MRI is not generally recommended as a screening tool by itself. For instance, in breast imaging, although it is a sensitive test, it may still miss some cancers that mammograms which use doses of ionizing radiation to create images would detect. Moreover it is more likely to find something that turns out not to be cancer (called a false positive). False-positive findings have to be checked out to make sure that the cancer isn't present, which results in coming back for further tests or biopsies. Also, MRI is more expensive than CT and Ultrasound.

Chapter 5

Microwave - Induced Thermoacoustic Imaging

Thermoacoustic tomography is a hybrid biomedical imaging modality, combining the high contrast and good tissue penetration of microwave and high spatial resolution of ultrasound imaging without harmful side effects. Firstly, it does not break, or change the properties of the biological tissue under study. Secondly, only nonionizing radiation is used. The non-destructive (non-invasive) and non-ionizing nature of thermoacoustic techniques makes them ideal for in vivo applications. Thirdly, the relationships between thermoacoustic signals and the physical parameters of biological tissues are well defined. The thermoacoustic wave generation is illustrated in Fig.5.1. In thermoacoustic wave generation, the

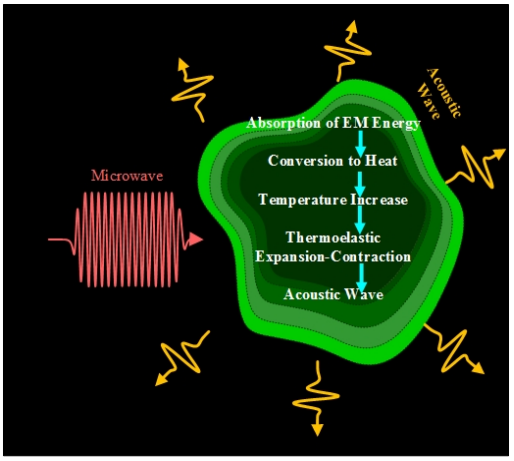

Figure 5.1: Schematic representation of thermoacoustic effect on tissue.

tissue is irradiated by pulsed microwave excitation; the microwave energy is selectively absorbed by different tissue structures with different dielectric parameters.

Then it is converted to heat pulse which causes generation of acoustic waves by thermoelastic expansion; the thermoacoustic signals are detected by ultrasound transducers to be used for image reconstruction of the mediums.

5.1 Solution Of The Thermoacoustic Wave Equation For Multi-Layer Planar Medium

The thermoacoustic wave equation is given as

$$\left(\nabla^2 - \frac{1}{c^2}\frac{\partial^2}{\partial t^2}\right) p(\mathbf{r}, t) = -\frac{\beta}{C_p}\frac{\partial H(\mathbf{r}, t)}{\partial t}, \tag{5.1}$$

which is called as inhomogeneous differential equation where $\mathbf{r} = (x, y, z)$ is the source location in the Cartesian coordinates, c is the propagation velocity of the wave (positive constant), $p(\mathbf{r}, t)$ is the acoustic wave function ($p(\mathbf{r}, t) \in \mathbb{C}^2(\mathbb{R}^3 \times \mathbb{R})$). $H(\mathbf{r}, t)$ is the heat function given by $\frac{\beta}{\kappa c^2}\frac{\partial T(\mathbf{r}, t)}{\partial t}$. T is the temperature rise, and β is the thermal coefficient of volume expansion (isobaric volume expansion coefficient). Here, we have the isothermal compressibility using the equation $\kappa c^2 = \frac{C_p}{C_v \rho}$ where C_p and C_v specific heat capacities at constant pressure and volume, respectively and ρ is the density of medium. The thermal energy converted per unit volume and per unit time and given by $H(\mathbf{r}, t) = A(\mathbf{r})I(t)$ where $A(\mathbf{r})$ spatial absorption function and $I(t)$ is a nonnegative function under the condition of thermal confinement which is given in Chapter 3. $I(t)$'s integration over time equals the pulse energy, $I(t) = \delta(t)$ where $\delta(.)$ is the Dirac delta function. Also $p_0(\mathbf{r}) = \Gamma A(\mathbf{r})$ where $\Gamma = \beta/(\kappa\rho C_v)$ is the Grueneisen parameter. Using these, we can rewrite (5.1) as

$$\left(\nabla^2 - \frac{1}{c^2}\frac{\partial^2}{\partial t^2}\right) p(\mathbf{r}, t) = -p_0(\mathbf{r})\frac{\partial \delta(t)}{\partial t}. \tag{5.2}$$

The left-hand side of (5.2) describes the wave propagation, whereas the right-hand side represents the source term.

5.1.1 Multi-Layer Tissue Model

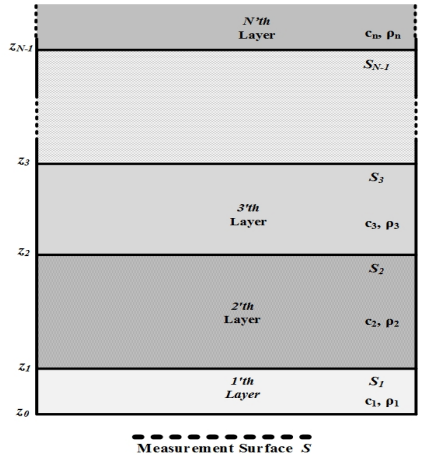

Figure 5.2: Geometrical representation of $N-$layer planar medium.

The y cross-section of multi-layer (N-layer) planar medium defined in $\mathbb{R}^3$ are shown in Fig. 5.2, where the acoustic detection is performed on the outer surface of the first layer.

In Fig. 5.2, we consider that the velocity c_m and the density ρ_m indicate the values of $c_m(\mathbf{r})$ and $\rho_m(\mathbf{r})$ between the mth and $(m-1)$th layers. Density and velocity in each layer are constants, while the layer thickness can be different ($m \leq N$). S_m is the mth layer boundary surface. We assume that there is another line S'_m(parallel to S_m) at infinity and also that the combination of S'_m and S_m encloses the source inside ($m = 1, ..., N$). For convenience, we define $S = S'_m + S_m$. The y cross-section of the planar medium modelled by N-parallel layers with different acoustic properties is given in Fig. 5.2, where the acoustic detection is performed on the outer surface of the first layer. Note that the N-th layer extents from z_{N-1} to ∞. For the multi-layer planar model, the inverse source problem is to obtain the source distribution in all of the layers using the acoustic data measured by the transducers. Thermoacoustic imaging is based on the inverse solution of the inhomogeneous acoustic wave equation with initial condition, boundary conditions at layers, and radiation conditions at infinity. The

solution to thermoacoustic problem can be used for any layered biological tissue as breast model in Fig. 5.3.

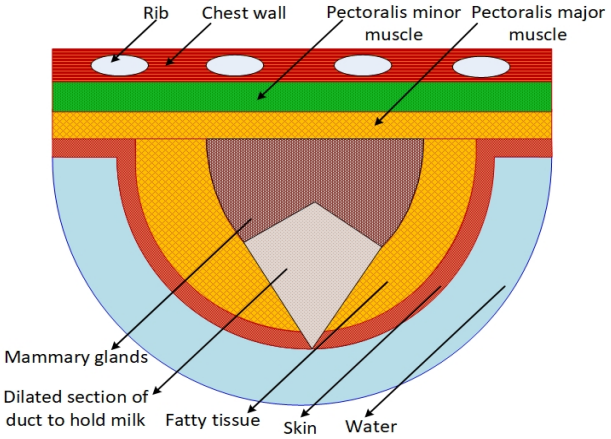

Figure 5.3: Layered breast model

Also the solution to thermoacoustic problem can be used for biological tissue as skin model in Fig. 5.4.

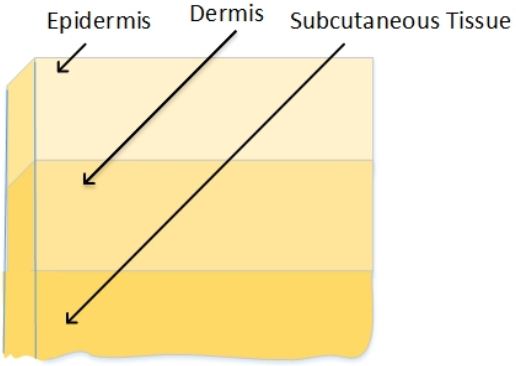

Figure 5.4: Layered skin model

Since the Fourier transformation provides a great deal of convenience for deriving the solution of the (5.2), we take the temporal Fourier transform of both sides of (5.2) in the first step as follows:

$$\nabla^2 P(\mathbf{r},\omega) + k_m^2 P(\mathbf{r},\omega) = iwp_0^{(m)}(\mathbf{r}). \tag{5.3}$$

We obtain Helmholtz equation after taking the temporal Fourier transform of (5.2). Here, ω is the temporal frequency coordinate, $k_m = \omega/c_m$ is the wave number in the mth layer where m indicates the source location, and $p_0^{(m)}$ represents the source function in the mth layer. First, we derive the forward solution of (5.3), and then we derive the inverse solution of (5.3).

In next section, we shall define the radiation conditions, continuity conditions on the boundary surface, and the initial condition for (5.3).

5.1.2 Radiation Conditions, Continuity Conditions And Initial Condition

The radiation conditions:
The radiation condition for $P(\mathbf{r}, \omega)$ are defined as

$$P(\mathbf{r}, \omega) = O(1/ \mid \mathbf{r} \mid) \quad as \mid \mathbf{r} \mid \to \infty \tag{5.4}$$

and

$$\frac{\partial P}{\partial \mid \mathbf{r} \mid}(\mathbf{r}, \omega) - ikP(\mathbf{r}, \omega) = o(1/ \mid \mathbf{r} \mid) \quad as \mid \mathbf{r} \mid \to \infty. \tag{5.5}$$

We use the Green's function which is a type of function used to solve inhomogeneous differential equations in (5.3) subject to boundary conditions. Green's function, which is represented as $G(\mathbf{r}, \mathbf{r}')$, is the response function at $\mathbf{r}$ due to a concentrated source at $\mathbf{r}'$.

Because of the important roles in the forward and inverse solution derivation of (5.2), we define the outcoming Green's function in which the wave propagates in the direction $\mathbf{r}' \to \mathbf{r}$ and incoming Green's function in which the wave propagates in the direction $\mathbf{r} \to \mathbf{r}'$. Outcoming and incoming waves are represented by the superscripts "out" and "in" for Green's function respectively. These functions also satisfies radiation conditions as follows:

$$G^{\text{out}}(R,\omega) = O(1/R) \quad as \quad R \to \infty, \quad R = \mid \mathbf{r} - \mathbf{r}^{'} \mid \tag{5.6}$$

and

$$\frac{\partial G^{\text{out}}}{\partial R} + ikG^{\text{out}} = o(1/R^2) \quad as \quad R \to \infty, \tag{5.7}$$

$$G^{\text{in}}(R,\omega) = O(1/R) \quad as \quad R \to \infty, \quad R = \mid \mathbf{r} - \mathbf{r}^{'} \mid \tag{5.8}$$

and

$$\frac{\partial G^{\text{in}}}{\partial R} - ikG^{\text{in}} = o(1/R^2) \quad as \quad R \to \infty. \tag{5.9}$$

Continuity conditions:

The boundary conditions for layered medium outlined below are based on well-known conditions used for solutions of wave equations. These conditions are named continuity conditions. The continuity at each layer boundary surface S_m is defined by the following for acoustic wave function.

$$\lim_{\mathbf{r}\to S_m^-} P(\mathbf{r},\omega) = \lim_{\mathbf{r}\to S_m^+} P(\mathbf{r},\omega), \tag{5.10}$$

and

$$\lim_{\mathbf{r}\to S_m^-} \frac{1}{\rho_{m-1}} \frac{\partial P(\mathbf{r},\omega)}{\partial \mathbf{n}} = \lim_{\mathbf{r}\to S_m^+} \frac{1}{\rho_m} \frac{\partial P(\mathbf{r},\omega)}{\partial \mathbf{n}}, \tag{5.11}$$

where, P is the acoustic waves which is generated by the source in the mth layer. Here, ρ_{m-1} and ρ_m are the densities for the layers $(m-1)$ and m, respectively and $\mathbf{n}$ is the normal of the layer surface and detection surface.

$G(\mathbf{r}^{'}, \mathbf{r}, \omega)$ also satisfies the continuity conditions on the layer boundaries. We represent it as follows:

$$\lim_{\mathbf{r}\to S_m^-} G(\mathbf{r}^{'}, \mathbf{r}, \omega) = \lim_{\mathbf{r}\to S_m^+} G(\mathbf{r}^{'}, \mathbf{r}, \omega), \tag{5.12}$$

and

$$\lim_{\mathbf{r}\to S_m^-} \frac{1}{\rho_{m-1}} \frac{\partial G(\mathbf{r}^{'}, \mathbf{r}, \omega)}{\partial \mathbf{n}} = \lim_{\mathbf{r}\to S_m^+} \frac{1}{\rho_m} \frac{\partial G(\mathbf{r}^{'}, \mathbf{r}, \omega)}{\partial \mathbf{n}}. \tag{5.13}$$

Also, continuity conditions at layer boundaries are satisfied by the outcoming and incoming Green's function.

Initial Condition at $\mathbf{t = 0}$:

The inhomogeneous thermoacoustic wave equation (5.2) must also satisfy the following initial condition

$$p(\mathbf{r}, t = 0) = p_0(\mathbf{r}). \tag{5.14}$$

5.1.3 Forward Solution

In forward solution of (5.3), we find the pressure field at the measurement surface assuming that we know the source function $p_0^{(m)}(\mathbf{r})$ in (5.3). For an arbitrary layer, say mth layer, given the source density $p_0^{(m)}(\mathbf{r})$, we need to find the acoustic wave function $P(\mathbf{r}, \omega)$ for all $\mathbf{r} \in \mathbb{R}^3$ in frequency domain. Some functional relations are valid between incoming with outcoming waves with negative and positive frequencies for $G^{\text{out}}(\mathbf{r}', \mathbf{r}, \omega)$ and $G^{\text{in}}(\mathbf{r}^{'}, \mathbf{r}, \omega)$ as follows:

$$G^{\text{out}}(\mathbf{r}^{'}, \mathbf{r}, \omega) = G^{\text{in}}(\mathbf{r}^{'}, \mathbf{r}, -\omega) \tag{5.15}$$

$$G^{\text{out}}(\mathbf{r}^{'}, \mathbf{r}, -\omega) = (G^{\text{out}}(\mathbf{r}^{'}, \mathbf{r}, \omega))^* \tag{5.16}$$

where * denotes the complex conjugate.

We call $G^{\text{out}}(\mathbf{r}^{'}, \mathbf{r}, \omega) \equiv G^{\text{out}}(\mathbf{r}^{'}, \mathbf{r})$ for simplicity, and

$$\nabla^2 G(\mathbf{r}^{'}, \mathbf{r}) + k^2 G(\mathbf{r}^{'}, \mathbf{r}) = -\delta(\mathbf{r} - \mathbf{r}^{'}), \tag{5.17}$$

which is written in terms of Green's function [33]. Here, $\mathbf{r}$ and $\mathbf{r}^{'}$ denote the observation (measurement) and source locations for N layer planar medium, respectively.

Noticing that the Dirac delta function is even,

$$\delta(-\mathbf{r}) = \delta(\mathbf{r}), \tag{5.18}$$

The equation (5.17) is satisfied for the incoming and outcoming Green's functions for any mth layer. As such,

$$\nabla^2 G^{\text{out}}(\mathbf{r}^{'}, \mathbf{r}) + k_m^2 G^{\text{out}}(\mathbf{r}^{'}, \mathbf{r}) = -\delta^{(m)}(\mathbf{r} - \mathbf{r}^{'}). \tag{5.19}$$

We know the following from the equation (5.3).

$$\nabla^2 P + k_m^2 P \;\; = \;\; iwp_0(\mathbf{r}'). \tag{5.20}$$

If we multiply P and G^{out} and by (5.19) and (5.20) respectively, and substract side by side, we obtain

$$G^{\text{out}} \nabla^2 P - P \nabla^2 G^{\text{out}} = P\delta(\mathbf{r} - \mathbf{r}') + iwp_0(\mathbf{r}')G^{\text{out}}, \tag{5.21}$$

which is valid in $\mathbf{R^3}$. If we integrate (5.21) in a very large circle of radius $\mathbf{R}'$, which involves the source inside, then we write,

$$\begin{aligned}&\int_{|\mathbf{r}'|\leq\mathbf{R}'}\left\{G^{\text{out}}(\mathbf{r}',\mathbf{r})\nabla^2 P(\mathbf{r}',\omega)-P(\mathbf{r}',\omega)\nabla^2 G^{\text{out}}(\mathbf{r}',\mathbf{r})\right\}d\mathbf{r}'\\&=\int_{V_0^{(m)}}P(\mathbf{r}',\omega)\delta(\mathbf{r}-\mathbf{r}')d\mathbf{r}'+iw\int_{V_0^{(m)}}p_0(\mathbf{r}')G^{\text{out}}(\mathbf{r}',\mathbf{r})d\mathbf{r}'.\end{aligned}\tag{5.22}$$

By applying the classical Green's formula to equation (5.22), we get

$$\begin{aligned}&\int_{\mathbb{R}'}\left\{G^{\text{out}}(\mathbf{r}',\mathbf{r})\frac{\partial}{\partial\mathbf{n}}P(\mathbf{r}',\omega)-P(\mathbf{r}',\omega)\frac{\partial}{\partial\mathbf{n}}G^{\text{out}}(\mathbf{r}',\mathbf{r})\right\}dS\\&=iw\int_{V_0^{(m)}}p_0(\mathbf{r}')G^{\text{out}}(\mathbf{r}',\mathbf{r})d\mathbf{r}'+P(\mathbf{r},\omega).\end{aligned}\tag{5.23}$$

Now let us make $\mathbf{R}'\to\infty$, consider the radiation conditions satisfied by P and G^{out}. Due to the factor $\mathbf{R}'^2$ existing in the surface element dS, the left hand side tends to zero and yields,

$$P(\mathbf{r},\omega)=-iw\int_{V_0^{(m)}}p_0(\mathbf{r}')G^{\text{out}}(\mathbf{r}',\mathbf{r})d\mathbf{r}'.\tag{5.24}$$

Let us call $V_0^{(m)}=V^{(m)}$ for simplicity. Here, $V^{(m)}$ represents the volume which encloses the source in the mth layer. The first and the second subscripts of $G_{ms}^{\text{out}}(\mathbf{r}',\mathbf{r})$ denote the source layer and measurement surface respectively. In physically, $G_{ms}^{\text{out}}(\mathbf{r}',\mathbf{r})$ refers to the pressure field on the measurement surface which is coming from the layer where the source is. In our derivations, we consider $w>0$ and $P(\mathbf{r},w)$ corresponding to the outcoming wave. If we assume that the source is in the all layers, we represent the forward solution as follows:

$$P(\mathbf{r},\omega)=-i\omega\sum_{m=1}^{N}\int_{V^{(\text{m})}}p_0^{(\text{m})}(\mathbf{r}')G_{ms}^{\text{out}}(\mathbf{r}',\mathbf{r})d\mathbf{r}'.\tag{5.25}$$

5.1.4 Coefficients Of The Green's Functions

When we write $\mathbf{r}' = (x', y', z')$ and $\mathbf{r} = (x, y, z)$ in (5.17), we obtain

$$\begin{aligned}&\nabla^2 G_m^{\text{out}}(x', y', z'; x, y, z) + k_m^2 G_m^{\text{out}}(x', y', z'; x, y, z)\\ &= -\delta^{(m)}(x - x')\delta^{(m)}(y - y')\delta^{(m)}(z - z').\end{aligned} \tag{5.26}$$

Here, we denote by $\hat{G}^{\text{out}}$ the two dimensional spatial Fourier transform of G^{out}:

$$\hat{G}^{\text{out}}(k_x, k_y, z; x', y', z') = \iint_{-\infty}^{\infty} G^{\text{out}}(\mathbf{r}, \mathbf{r}') exp(-i(k_x x + k_y y))dxdy \tag{5.27}$$

$$G^{\text{out}}(x, y, z; x', y', z') = \frac{1}{(2\pi)^2} \iint_{-\infty}^{\infty} \hat{G}^{\text{out}}(k_x, k_y, z; \mathbf{r}') \exp(i(k_x x + k_y y))dk_x dk_y \tag{5.28}$$

where k_x and k_y are spatial frequency, and, $\mathbf{r} = (x, y, z)$ and $\mathbf{r}' = (x', y', z')$ are the measurement and the source coordinates respectively. When we take the two-dimensional spatial Fourier transform in x and y directions of the equation (5.26), we get

$$\begin{aligned}&\iint_{-\infty}^{\infty} \left(\nabla^2 G_m^{\text{out}} + k_m^2 G_m^{\text{out}}\right) \exp(-i(k_x + k_y))dxdy\\ &= \quad -\iint_{-\infty}^{\infty} \delta^{(m)}(x - x')\delta^{(m)}(y - y')\delta^{(m)}(z - z') \exp(i(k_x x + k_y y))dxdy.\end{aligned} \tag{5.29}$$

As a result,

$$\frac{\partial^2 \hat{G}_m^{\text{out}}}{\partial z^2} + k_m^2 \hat{G}_m^{\text{out}} - (k_x^2 + k_y^2)\hat{G}_m^{\text{out}} = -\exp(-i(k_x x' + k_y y'))\delta^{(m)}(z - z'). \tag{5.30}$$

We can write the equation (5.30) as in the following form

$$\frac{\partial^2 \hat{G}_m^{\text{out}}}{\partial z^2} - k_z^{2(m)} \hat{G}_m^{\text{out}} = -\exp(-i(k_x x' + k_y y'))\delta^{(m)}(z - z'). \tag{5.31}$$

Here, k_x, k_y and $k_z^{(m)}$ are the spatial frequency components of the wave vector for the mth layer, and $k_z^{(m)}$ is expressed as

$$k_z^{(m)} = \begin{cases} -i\sqrt{\left(\frac{\omega}{c_m}\right)^2 - (k_x^2 + k_y^2)}, & \left|\frac{\omega}{c_m}\right| > \sqrt{k_x^2 + k_y^2} \\ \sqrt{(k_x^2 + k_y^2) - \left(\frac{\omega}{c_m}\right)^2}, & \sqrt{k_x^2 + k_y^2} > \left|\frac{\omega}{c_m}\right|. \end{cases} \tag{5.32}$$

The first term of the right hand side of (5.31) is derived from the jump discontinuity at the source location which is given step by step as the follows.

Jump Discontinuities At Source Location

Snce the right hand side of (5.31) has impulsive source at $z' = z$, both $\hat{G}^{\text{out}}(\mathbf{r}', \mathbf{r})$ and $\hat{G}^{\text{in}}(\mathbf{r}', \mathbf{r})$ have jump discontinuities at $\mathbf{r}' = \mathbf{r}$ (i.e. $z' = z$) which is in the mth layer. The Green's function $\hat{G}_m^{\text{out}}(\mathbf{r}', \mathbf{r})$ is continuous at $z = z'$. However, $\dfrac{\partial \hat{G}_m^{\text{out}}}{\partial z}$ is not continuous at $z = z'$, and it has a jump discontinuity obtained by integrating the differential equation (5.31) from $z = z' - \epsilon$ to $z = z' + \epsilon$, the amount of discontinuities equal to $-e^{-i(k_x x' + k_y y')}$. If we integrate from $z' - \epsilon$ to $z' + \epsilon$, we obtain

$$\lim_{\epsilon \to 0} \int_{z'-\epsilon}^{z'+\epsilon} \frac{\partial^2 \hat{G}_m^{\text{out}}}{\partial z^2} dz = \lim_{\epsilon \to 0} k_z^{2(m)} \int_{z'-\epsilon}^{z'+\epsilon} \hat{G}_m^{\text{out}} dz - e^{-i(k_x x' + k_y y')} \lim_{\epsilon \to 0} \int_{z'-\epsilon}^{z'+\epsilon} \delta(z - z') dz. \tag{5.33}$$

Since the Green's function is continuous at $z = z'$, the first term of right hand side of (5.33) is equal to

$$\lim_{\epsilon \to 0} k_z^{2(m)} \int_{z'-\epsilon}^{z'+\epsilon} \hat{G}_m^{\text{out}} dz = 0. \tag{5.34}$$

Then, (5.33) may also be given by

$$\lim_{\epsilon \to 0} \left[\frac{\partial \hat{G}_m^{\text{out}}}{\partial z} \Big|_{z=z'+\epsilon} - \frac{\partial \hat{G}_m^{\text{out}}}{\partial z} \Big|_{z=z'-\epsilon} \right] = -e^{-i(k_x x' + k_y y')}. \tag{5.35}$$

The differential equation (5.31) is reduced to the homogeneous form

$$\frac{\partial^2 \hat{G}_m^{\text{out}}}{\partial z^2} - k_z^{2^{(m)}} \hat{G}_m^{\text{out}} = 0 \tag{5.36}$$

which is separable differential equation except the case when the source is at $z' = z$. We express the Green's function in (5.36) for mth layer as the following.

$$\hat{G}_m^{\text{out}} = \begin{cases} C_1 e^{k_z^{(1)} z} + C_2 e^{-k_z^{(1)} z}, & 0 \leq z \leq z_1 \\ C_3 e^{k_z^{(2)} z} + C_4 e^{-k_z^{(2)} z}, & z_1 \leq z \leq z_2 \\ \quad . & \quad . \\ \quad . & \quad . \\ \quad . & \quad . \\ C_{2m-1} e^{k_z^{(m)} z} + C_{2m} e^{-k_z^{(m)} z}, & z_{m-1} \leq z' \leq z \leq z_m \\ C_{2m+1} e^{k_z^{(m)} z} + C_{2m+2} e^{-k_z^{(m)} z}, & z_{m-1} \leq z \leq z' \leq z_m \\ \quad . & \quad . \\ \quad . & \quad . \\ \quad . & \quad . \\ C_{2N+1} e^{k_z^{(N)} z} + C_{2N+2} e^{-k_z^{(N)} z}, & z_{N-1} \leq z < \infty. \end{cases} \tag{5.37}$$

We may find the coefficients by solving the differential equations for the $N-$ layer planar geometry assuming the source is in the $m-$th layer by using continuity conditions on the layer boundaries, radiation conditions at infinity and the jump discontinuity at source location. We write the system of linear equations for (5.31)

as follows:

$$\begin{bmatrix} A_0 & & & & & \\ A_{11} & A_{12} & & & & \\ & A_{21} & A_{22} & & & \\ & \ddots & \ddots & & 0'_s & \\ & & A_{j1} & A_{j2} & & \\ & & & \ddots & \ddots & \\ & 0'_s & & & & \\ & & & & & A_N \end{bmatrix} \times \begin{bmatrix} C_1 \\ \vdots \\ C_{2N+2} \end{bmatrix} = \begin{bmatrix} 0 \\ \vdots \\ -e^{-i(k_x x' + k_y y')} \\ 0 \\ \vdots \end{bmatrix}. \tag{5.38}$$

Here, the matrix on the left is a $(2N+2) \times (2N+2)$ square matrix. By using the radiation conditions, we write the following elements

$$A_0 = A_N = [1].$$

Using the continuity conditions on the layer boundaries, we obtain

$$A_{j1} = \begin{bmatrix} a_{j1} & a_{j2} \\ \frac{\rho_{j+1}}{\rho_j} b_{j1} & \frac{\rho_{j+1}}{\rho_j} b_{j2} \end{bmatrix} \quad \text{and} \quad A_{j2} = \begin{bmatrix} a_{j3} & a_{j4} \\ b_{j3} & b_{j4} \end{bmatrix}. \tag{5.39}$$

where ρ_j indicates the density of the medium in the jth layer ($j = 1, ..., N-1$). We can write the explicit expressions of the elements of the matrices A_{j1} and A_{j2} as follows:

$$a_{j1} = e^{k_z^{(j)} l_j} \qquad b_{j1} = k_z^{(j)} e^{k_z^{(j)} l_j} \tag{5.40}$$

$$a_{j2} = e^{-k_z^{(j)} l_j} \qquad b_{j2} = -k_z^{(j)} e^{-k_z^{(j)} l_j} \tag{5.41}$$

$$a_{j3} = -e^{k_z^{(j+1)} l_j} \qquad b_{j3} = -k_z^{(j+1)} e^{k_z^{(j+1)} l_j} \tag{5.42}$$

$$a_{j4} = -e^{-k_z^{(j+1)} l_j} \qquad b_{j4} = k_z^{(j+1)} e^{-k_z^{(j+1)} l_j} \tag{5.43}$$

where

$$k_z^{(j)} = \sqrt{\left(\frac{\omega}{c_j}\right)^2 - (k_x^2 + k_y^2)}. \tag{5.44}$$

Here, c_j (positive constant) is the propagation velocity of the wave which is in the jth medium, l_j is the layer coordinate which gives the layer information, ω is the temporal frequency,and k_x and k_y are the spatial frequency at x and y direction, respectively. Also, we have the following which includes $2m$th and $(2m+1)$th row elements supposing the source is in the mth layer:

$$A_{m1} = \begin{bmatrix} l_1 & l_2 \\ d_1 & d_2 \end{bmatrix}, \quad A_{m2} = \begin{bmatrix} -l_1 & -l_2 \\ -d_1 & -d_2 \end{bmatrix}. \tag{5.45}$$

Because of the jump discontinuity at the source location, l_1, l_2, d_1, d_2 are written as follows:

$$\begin{aligned} l_1 &= e^{k_z^{(m)} z'}, & l_2 &= e^{-k_z^{(m)} z'} \\ d_1 &= k_z^{(m)} e^{k_z^{(m)} z'}, & d_2 &= -k_z^{(m)} e^{-k_z^{(m)} z'} \end{aligned}$$

where z' is the source location on the axis of z.

The coefficent matrix of the linear system of equation's in (5.38) is written as the following which is called C:

$$C = \begin{bmatrix} C_1 \\ \vdots \\ C_{2N+2} \end{bmatrix}. \tag{5.46}$$

Here, elements of the matrix C represent the coefficients of the Green's function generated by the source in the mth layer associated with the boundary conditions, jump discontinuities at source locations, and the radiation conditions at infinity.

We denote the matrix in the right hand side of the linear system of equation's in (5.38) by B:

$$B = \begin{bmatrix} 0 \\ \vdots \\ -e^{-i(k_x x' + k_y y')} \\ 0 \\ \vdots \end{bmatrix}, \tag{5.47}$$

Dimension of the matrix B is $(2N+2) \times 1$. Because of the jump discontinuities in the source location, the only nonzero element is $-e^{-i(k_x x' + k_y y')}$, located at the $(2m+1)$th row in (5.47).

The determinant of the first matrix in (5.38) is

$$\begin{vmatrix} A_0 & & & & & & \\ A_{11} & A_{12} & & & & & \\ & A_{21} & A_{22} & & & & \\ & \ddots & \ddots & & & 0'_s & \\ & & A_{j1} & A_{j2} & & & \\ & & & \ddots & \ddots & & \\ & 0'_s & & & & & \\ & & & & & A_N & \end{vmatrix}. \tag{5.48}$$

By means of the row operations in (5.48), we obtain

$$= -2k_z^{(m)} \begin{vmatrix} A_0 & & & & & & \\ A_{11} & A_{12} & & & & & \\ & A_{21} & A_{22} & & & & \\ & \ddots & \ddots & & & 0'_s & \\ & & A_{j1} & A_{j2} & & & \\ & & & \ddots & \ddots & & \\ & 0'_s & & & & & \\ & & & & & A_N & \end{vmatrix}. \tag{5.49}$$

We can find the coefficients by solving the differential equations for the $N-$ layer planar geometry assuming the source is in the mth layer. The system of linear equations may be given by $[A].\vec{C} = \vec{B}$. If we write $\mid A \mid = -2k_z^{(m)} \mid a \mid$, and apply the cofactor expansion along the $(2m+1)$th row and column the determinant of a depends only layer informations, spatial frequency and the temporal frequency, not where the source is. $\vec{C}$ is a vector whose elements are the coefficients of the Green's functions described by $C = [C_1, C_2, \cdots, C_{2N+2}]$ in (5.46). $\vec{B}$ is a vector which includes $2N+2$ elements and these elements are zero except only one element. The nonzero element is -$e^{-i(k_x x' + k_y y')}$ in (5.47). Also, $\vec{B}$ depends on the layer which includes the source location. When we write the explicit form of these matrices, because of definition of the k_z, the coefficients of Green's functions will be even functions of temporal frequency . In order to specify the Green's function the unknown coefficients C_{2N+1} must be determined, which can be done by using the Cramer's Rule.

After solving the equation (5.36) for the N-layer planar geometry and taking the inverse Fourier transform of the Green's function at x and y direction, respectively, we derive the outgoing Green's function $G_m^{\text{out}}(\mathbf{r}', \mathbf{r}) = G_m^{\text{out}}(x', y', z'; x, y, z)$ in Fourier domain which is generated by the source in the mth layer as follows:

$$G_m^{\text{out}} = \frac{1}{(2\pi)^2} \begin{cases} \int_{-\infty}^{\infty}\int_{-\infty}^{\infty} e^{ik_x(x-x')+ik_y(y-y')}(C_1 e^{k_z^{(1)}z} + C_2 e^{-k_z^{(1)}z})dk_x dk_y, \\ \qquad 0 \le z \le z_1 \\ \int_{-\infty}^{\infty}\int_{-\infty}^{\infty} e^{ik_x(x-x')+ik_y(y-y')}(C_3 e^{k_z^{(2)}z} + C_4 e^{-k_z^{(2)}z})dk_x dk_y, \\ \qquad z_1 \le z \le z_2 \\ \qquad \vdots \\ \int_{-\infty}^{\infty}\int_{-\infty}^{\infty} e^{ik_x(x-x')+ik_y(y-y')}(C_{2m-1} e^{k_z^{(m)}z} + C_{2m} e^{-k_z^{(m)}z})dk_x dk_y, \\ \qquad z_{m-1} \le z' \le z \le z_m \\ \int_{-\infty}^{\infty}\int_{-\infty}^{\infty} e^{ik_x(x-x')+ik_y(y-y')}(C_{2m+1} e^{k_z^{(m)}z} + C_{2m+2} e^{-k_z^{(m)}z})dk_x dk_y, \\ \qquad z_{m-1} \le z \le z' \le z_m \\ \qquad \vdots \\ \int_{-\infty}^{\infty}\int_{-\infty}^{\infty} e^{ik_x(x-x')+ik_y(y-y')}(C_{2N+1} e^{k_z^{(N)}z} + C_{2N+2} e^{-k_z^{(N)}z})dk_x dk_y, \\ \qquad z_{N-1} \le z < \infty. \end{cases} \tag{5.50}$$

The coefficients C_k ($1 \le k \le 2N+2$) are determined by solving $(2N+2)$ equations associated to the boundary conditions on the layer boundary, jump discontinuities at the source locations and radiation conditions at infinity. $G_{ms}^{\text{out}}(\mathbf{r}', \mathbf{r})$ (outcoming Green's function) which comes from the source to surface is represented by

$$\frac{1}{(2\pi)^2} \iint_{-\infty}^{\infty} C_{2N+1} e^{k_z^s z} e^{ik_x(x-x')+ik_y(y-y')} dk_x dk_y, \tag{5.51}$$

where s and m indicate the measurement surface and the source location, respectively.

5.1.5 Inverse Solution

Thermoacoustic image reconstruction based on inverse solution of thermoacoustic wave equation with homogeneous medium parameters have been studied by different researchers as mentioned in chapter 2.

The source distribution inside the medium has been determined by the following integral equation for the homogeneous medium [23]:

$$q(\mathbf{r}) = \frac{1}{\pi} \int_S \int_{-\infty}^{\infty} P(\mathbf{r_s}, \omega) \frac{\partial G_h^{\text{in}}(\mathbf{r}, \mathbf{r_s})}{\partial \mathbf{n}} d\omega dS, \tag{5.52}$$

where S is a measurement surface and G_h^{in} is a free space Green's function represented as $G_h^{\text{in}} = \frac{1}{4\pi} \frac{e^{-ikR}}{R}$, $R = \mid \mathbf{r} - \mathbf{r}' \mid$ and $\mathbf{n}$ is the normal along z-axis . $\mathbf{r_s}$ and $\mathbf{r}$ are the measurement and the source coordinate, respectively. $P(\mathbf{r_s}, \omega)$ is the measured pressure from the measurement surface defined as:

$$P(\mathbf{r_s}, \omega) = -i\omega \int_{V_0} p_0(\mathbf{r}) G^{\text{out}}(\mathbf{r}, \mathbf{r_s}) dV_0. \tag{5.53}$$

By using the inverse solution for the homogeneous medium, we derive the solution of the inverse source problem for N-layer planar medium with existing the source distribution in all layers where we use spatially continuous layered Green's function with parameters associated to the layers. $G^{\text{in}}(\mathbf{r}, \mathbf{r_s})$ and $G^{\text{out}}(\mathbf{r}', \mathbf{r_s})$ are symmetric with respect to the source and the measurement location parameters, and satisfy the Helmholtz equation. So we get

$$\nabla_s^2 G_{ij}^{\text{in}}(\mathbf{r_i}, \mathbf{r_s}) + k_i^2 G_{ij}^{\text{in}}(\mathbf{r_i}, \mathbf{r_s}) = -\delta_{ij} \delta(\mathbf{r_i} - \mathbf{r_s}), \tag{5.54}$$

$$\nabla_s^2 G_{ij}^{\text{out}}(\mathbf{r_i'}, \mathbf{r_s}) + k_i^2 G_{ij}^{\text{out}}(\mathbf{r_i'}, \mathbf{r_s}) = -\delta_{ij} \delta(\mathbf{r_i'} - \mathbf{r_s}), \tag{5.55}$$

where δ_{ij} is Kronecker delta and $i, j = 1, ..., N$. If we multiply (5.54) and (5.55) by G_{ij}^{out} and G_{ij}^{in} respectively, we obtain

$$\begin{aligned} & G_{ij}^{\text{out}}(\mathbf{r_i'}, \mathbf{r_s}) \nabla_s^2 G_{ij}^{\text{in}}(\mathbf{r_i}, \mathbf{r_s}) \\ & \quad = G_{ij}^{\text{in}}(\mathbf{r_i}, \mathbf{r_s}) \nabla_s^2 G_{ij}^{\text{out}}(\mathbf{r_i'}, \mathbf{r_s}) + \delta_{ij} G_{ij}^{\text{in}}(\mathbf{r_i}, \mathbf{r_s}) \delta(\mathbf{r_i'} - \mathbf{r_s}) \\ & \quad\quad - \delta_{ij} G_{ij}^{\text{out}}(\mathbf{r_i'}, \mathbf{r_s}) \delta(\mathbf{r_i} - \mathbf{r_s}) \end{aligned} \tag{5.56}$$

after substraction. If we add the term

$$G_{ij}^{\text{out}}(\mathbf{r_i'}, \mathbf{r_s}) \nabla_s^2 G_{ij}^{\text{in}}(\mathbf{r_i}, \mathbf{r_s}) + 2 \nabla_s G_{ij}^{\text{out}}(\mathbf{r_i'}, \mathbf{r_s}) \nabla_s G_{ij}^{\text{in}}(\mathbf{r_i}, \mathbf{r_s}) \tag{5.57}$$

to the both sides of (5.56), we get

$$\begin{aligned} & 2 G_{ij}^{\text{out}}(\mathbf{r_i'}, \mathbf{r_s}) \nabla_s^2 G_{ij}^{\text{in}}(\mathbf{r_i}, \mathbf{r_s}) + 2 \nabla_s G_{ij}^{\text{out}}(\mathbf{r_i'}, \mathbf{r_s}) \nabla_s G_{ij}^{\text{in}}(\mathbf{r_i}, \mathbf{r_s}) \\ & = G_{ij}^{\text{in}}(\mathbf{r_i}, \mathbf{r_s}) \nabla_s^2 G_{ij}^{\text{out}}(\mathbf{r_i'}, \mathbf{r_s}) + G_{ij}^{\text{out}}(\mathbf{r_i'}, \mathbf{r_s}) \nabla_s^2 G_{ij}^{\text{in}}(\mathbf{r_i}, \mathbf{r_s}) \\ & \quad + 2 \nabla_s G_{ij}^{\text{out}}(\mathbf{r_i'}, \mathbf{r_s}) \nabla_s G_{ij}^{\text{in}}(\mathbf{r_i}, \mathbf{r_s}) \\ & \quad + \delta_{ij} G_{ij}^{\text{in}}(\mathbf{r_i}, \mathbf{r_s}) \delta(\mathbf{r_i'} - \mathbf{r_s}) - \delta_{ij} G_{ij}^{\text{out}}(\mathbf{r_i'}, \mathbf{r_s}) \delta(\mathbf{r_i} - \mathbf{r_s}) \\ & = \nabla_s . \left(\nabla_s \left(G_{ij}^{\text{out}}(\mathbf{r_i'}, \mathbf{r_s}) G_{ij}^{\text{in}}(\mathbf{r_i}, \mathbf{r_s}) \right) \right) \\ & \quad + \delta_{ij} G_{ij}^{\text{in}}(\mathbf{r_i}, \mathbf{r_s}) \delta(\mathbf{r_i'} - \mathbf{r_s}) - \delta_{ij} G_{ij}^{\text{out}}(\mathbf{r_i'}, \mathbf{r_s}) \delta(\mathbf{r_i} - \mathbf{r_s}). \end{aligned} \tag{5.58}$$

Assuming that the source distribution is in all layers, we find the source in mth layer and these relations make easy to derive the inverse solution.

We claim that the following integral equation is valid as the inverse solution of the thermoacoustic wave equation for the $N-$ layer planar medium to find the source in the mth layer ($m \leq N$)

$$q(\mathbf{r}) = \frac{1}{\pi} \frac{\rho_m}{\rho_s} \int_S \int_{-\infty}^{\infty} P(\mathbf{r_s}, \omega) \frac{\partial G_{ms}^{\text{in}}(\mathbf{r}, \mathbf{r_s})}{\partial \mathbf{n}} d\omega dS \tag{5.59}$$

where $\mathbf{r'}$ and $\mathbf{r_s}$ are the source and the measurement locations respectively, ρ is the medium density, and the subscripts m and s indicate the layer which include the source and the measurement surface respectively. For the proof of (5.59),

using (5.25), we write

$$
\begin{aligned}
q(\mathbf{r}) = & -\frac{\rho_m}{\rho_s}\frac{i}{\pi}\int_{-\infty}^{\infty}\omega\int_S\left(\sum_{k=1}^{N}\int_{V^{(k)}} p_0^{(\mathrm{k})}(\mathbf{r}^{'})G_{ks}^{\mathrm{out}}(\mathbf{r}',\mathbf{r_s})d\mathbf{r}'\right)\\
& .\frac{\partial G_{ms}^{\mathrm{in}}(\mathbf{r},\mathbf{r_s})}{\partial\mathbf{n}}d\omega dS\\
= & -\frac{\rho_m}{\rho_s}\frac{i}{\pi}\sum_{k=1}^{N}\int_{V^{(k)}} p_0^{(k)}(\mathbf{r}^{'})\\
& .\left(\int_{-\infty}^{\infty}\omega\int_S G_{ks}^{\mathrm{out}}(\mathbf{r}',\mathbf{r_s})\nabla_s G_{ms}^{\mathrm{in}}(\mathbf{r},\mathbf{r_s})\mathbf{n}dSd\omega\right)d\mathbf{r}', \qquad (5.60)
\end{aligned}
$$

where $V^{(k)}$ is the volume which includes the source. If we call the terms with integrations over ω as $K(\mathbf{r}',\mathbf{r})$ and substitute $K(\mathbf{r}',\mathbf{r})$ in (5.60), we get

$$
q(\mathbf{r}) = -\frac{\rho_m}{\rho_s}\frac{1}{\pi}\sum_{k=1}^{N}\left[\int_{V^{(k)}} p_0^{(k)}(\mathbf{r}')K_k(\mathbf{r}',\mathbf{r})d\mathbf{r}'\right]. \qquad (5.61)
$$

For the mth layer, we take
$K_m(\mathbf{r}',\mathbf{r}) = K_m^{(1)}(\mathbf{r}',\mathbf{r}) + K_m^{(2)}(\mathbf{r}',\mathbf{r})$, where

$$
K_m^{(1)}(\mathbf{r},\mathbf{r}') = \int_{-\infty}^{\infty} i\omega\int_S G_{ms}^{\mathrm{out}}(\mathbf{r}',\mathbf{r_s})\nabla_s G_{ms}^{\mathrm{in}}(\mathbf{r},\mathbf{r_s})\mathbf{n}dSd\omega \qquad (5.62)
$$

$$
K_m^{(2)}(\mathbf{r},\mathbf{r}') = \int_{-\infty}^{\infty} i\omega\int_S G_{ks}^{\mathrm{out}}(\mathbf{r}',\mathbf{r_s})\nabla_s G_{ms}^{\mathrm{in}}(\mathbf{r},\mathbf{r_s})\mathbf{n}dSd\omega, \qquad (5.63)
$$

$k \neq m$ and $m,k \leq N$. We can rewrite the equation (5.62) by adding and subtracting the layer surfaces parallel to the measurement surface as follows:

$$
\begin{aligned}
K_m^{(1)}(\mathbf{r},\mathbf{r}') = & \int_{-\infty}^{\infty} i\omega\left(\int_S G_{ms}^{\mathrm{out}}(\mathbf{r}',\mathbf{r_s})\nabla_s G_{ms}^{\mathrm{in}}(\mathbf{r},\mathbf{r_s})\mathbf{n}dS\right.\\
& +\sum_{k=1}^{N}\left(\int_{S_k} G_{ms}^{\mathrm{out}}(\mathbf{r}',\mathbf{r_s})\nabla_s G_{ms}^{\mathrm{in}}(\mathbf{r},\mathbf{r_s})\right.\\
& \left.\left.-\int_{S_k} G_{ms}^{\mathrm{out}}(\mathbf{r}',\mathbf{r_s})\nabla_s G_{mS}^{\mathrm{in}}(\mathbf{r},\mathbf{r_s})\right)\right)\mathbf{n}dS_k d\omega. \qquad (5.64)
\end{aligned}
$$

Using the Divergence theorem and continuity conditions on the layer boundary, we get

$$K_m^{(1)}(\mathbf{r},\mathbf{r}') = \int_{-\infty}^{\infty} i\omega \sum_{k=1}^{N} \rho_k \left[\int_{V_k} \nabla_s (G_{mk}^{\text{out}}(\mathbf{r}',\mathbf{r_s}) \nabla_s G_{mk}^{\text{in}}(\mathbf{r},\mathbf{r_s})) dV_k \right] d\omega \tag{5.65}$$

Here, $\rho_k = \dfrac{\rho_s}{\rho(k)}, \quad k = 1, ..., N$, where ρ_s is the density of the measurement surface and $\rho(k)$ is the density of the medium k, we obtain these terms by using continuity conditions on the layer boundary. Both $G^{\text{out}}(\mathbf{r}',\mathbf{r_s})$ and $G^{\text{in}}(\mathbf{r},\mathbf{r_s})$ are scalar functions and we have the identity

$$\nabla_s \left(G^{\text{out}}(\mathbf{r}',\mathbf{r_s}) \nabla_s G^{\text{in}}(\mathbf{r},\mathbf{r_s}) \right) = \nabla_s G^{\text{out}}(\mathbf{r}',\mathbf{r_s}) \nabla_s G^{\text{in}}(\mathbf{r},\mathbf{r_s}) + G^{\text{out}} \nabla_s^2 G^{\text{in}}(\mathbf{r},\mathbf{r_s}). \tag{5.66}$$

Now using (5.58), (5.65), and (5.66), we have

$$
\begin{aligned}
K_m^{(1)}(\mathbf{r},\mathbf{r}') = &\int_{-\infty}^{\infty} i\omega\frac{\rho_s}{\rho_m}\int_{V^{(m)}}\big(\nabla_s G_{mm}^{\text{out}}(\mathbf{r}',\mathbf{r_s})\nabla_s G_{mm}^{\text{in}}(\mathbf{r},\mathbf{r_s})\\
&+ G_{mm}^{\text{out}}(\mathbf{r}',\mathbf{r_s})\nabla_s^2 G_{mm}^{\text{in}}(\mathbf{r},\mathbf{r_s})\big)\,dV_m d\omega\\
&+\int_{-\infty}^{\infty} i\omega\sum_{k=1,k\neq m}^{N}\rho_k\int_{V^{(k)}}\big(\nabla_s G_{mk}^{\text{out}}(\mathbf{r}',\mathbf{r_s})\nabla_s G_{mk}^{\text{in}}(\mathbf{r},\mathbf{r_s})\\
&+ G_{mk}^{\text{out}}(\mathbf{r}',\mathbf{r_s})\nabla_s^2 G_{mk}^{\text{in}}(\mathbf{r},\mathbf{r_s})\big)\,dV_k d\omega\\
=&\frac{\rho_s}{2\rho_m}\int_{-\infty}^{\infty} i\omega\int_{V_{(m)}}\big(\delta_{mm}\delta(\mathbf{r}'-\mathbf{r_s})G_{mm}^{\text{in}}(\mathbf{r},\mathbf{r_s})\\
&-\delta_{mm}\delta(\mathbf{r}-\mathbf{r_s})G_{mm}^{\text{out}}(\mathbf{r}',\mathbf{r_s})\big)\,dV_m d\omega\\
&+\frac{\rho_s}{2\rho_m}\int_{-\infty}^{\infty} i\omega\int_{V^{(m)}}\nabla_s.\left(\nabla_s\left(G_{mm}^{\text{out}}(\mathbf{r}',\mathbf{r_s})G_{mm}^{\text{in}}(\mathbf{r},\mathbf{r_s})\right)\right)dV_m d\omega\\
&+\frac{\rho_s}{2\rho_m}\int_{-\infty}^{\infty} i\omega\int_{V^{(m)}}\sum_{k=1,k\neq m}^{N}\big(\delta_{mk}\delta(\mathbf{r}'-\mathbf{r_s})G_{mk}^{\text{in}}(\mathbf{r},\mathbf{r_s})\\
&-\delta_{mk}\delta(\mathbf{r}-\mathbf{r_s})G_{mk}^{\text{out}}(\mathbf{r}',\mathbf{r_s})\big)\,dV_k d\omega\\
&+\int_{-\infty}^{\infty} i\omega\sum_{k=1,k\neq m}^{N}\frac{\rho_k}{2}\int_{V^{(k)}}\nabla_s.\left(\nabla_s\left(G_{mk}^{\text{out}}(\mathbf{r}',\mathbf{r_s})G_{mk}^{\text{in}}(\mathbf{r},\mathbf{r_s})\right)\right)dV_k d\omega.
\end{aligned}
\tag{5.67}
$$

In view of the definition of Kronecker delta, we can rewrite the equation (5.67) as

$$\begin{aligned}
K_m^{(1)}(\mathbf{r},\mathbf{r}') &= \int_{-\infty}^{\infty} i\omega\frac{\rho_s}{\rho_m}\int_{V^{(m)}}\big(\nabla_s G_{mm}^{\text{out}}(\mathbf{r}',\mathbf{r_s})\nabla_s G_{mm}^{\text{in}}(\mathbf{r},\mathbf{r_s}) \\
&\quad + G_{mm}^{\text{out}}(\mathbf{r}',\mathbf{r_s})\nabla_s^2 G_{mm}^{\text{in}}(\mathbf{r},\mathbf{r_s})\big)\,dV_m d\omega \\
&+ \int_{-\infty}^{\infty} i\omega\sum_{k=1,k\neq m}^{N}\rho_k\int_{V^{(k)}}\big(\nabla_s G_{mk}^{\text{out}}(\mathbf{r}',\mathbf{r_s})\nabla_s G_{mk}^{\text{in}}(\mathbf{r},\mathbf{r_s}) \\
&\quad + G_{mk}^{\text{out}}(\mathbf{r}',\mathbf{r_s})\nabla_s^2 G_{mk}^{\text{in}}(\mathbf{r},\mathbf{r_s})\big)\,dV_k d\omega \\
&= \frac{\rho_s}{2\rho_m}\int_{-\infty}^{\infty} i\omega\int_{V^{(m)}}\big(\delta(\mathbf{r}'-\mathbf{r_s})G_{mm}^{\text{in}}(\mathbf{r},\mathbf{r_s}) \\
&\quad - \delta(\mathbf{r}-\mathbf{r_s})G_{mm}^{\text{out}}(\mathbf{r}',\mathbf{r_s})\big)\,dV_m d\omega \\
&\quad + \frac{\rho_s}{2\rho_m}\int_{-\infty}^{\infty} i\omega\int_{V^{(m)}}\nabla_s.\left(\nabla_s\left(G_{mm}^{\text{out}}(\mathbf{r}',\mathbf{r_s})G_{mm}^{\text{in}}(\mathbf{r},\mathbf{r_s})\right)\right)dV_m d\omega \\
&\quad + \int_{-\infty}^{\infty} i\omega\sum_{k=1,k\neq m}^{N}\frac{\rho_k}{2}\int_{V^{(k)}}\nabla_s.\left(\nabla_s\left(G_{mk}^{\text{out}}(\mathbf{r}',\mathbf{r_s})G_{mk}^{\text{in}}(\mathbf{r},\mathbf{r_s})\right)\right)dV_k d\omega.
\end{aligned} \tag{5.68}$$

Let us take the fifth and the sixth line of (5.68)

$$\begin{aligned}
&\frac{\rho_s}{2\rho_m}\int_{-\infty}^{\infty} i\omega\int_{V^{(m)}}\big(\delta(\mathbf{r}'-\mathbf{r_s})G_{mm}^{\text{in}}(\mathbf{r},\mathbf{r_s}) - \delta(\mathbf{r}-\mathbf{r_s})G_{mm}^{\text{out}}(\mathbf{r}',\mathbf{r_s})\big)\,dV_m d\omega \\
&= \frac{\rho_s}{2\rho_m}\int_{-\infty}^{\infty} i\omega(G_{mm}^{\text{in}}(\mathbf{r},\mathbf{r}') - G_{mm}^{\text{out}}(\mathbf{r}',\mathbf{r}))d\omega
\end{aligned} \tag{5.69}$$

and use the forward solution, and the initial condition ($t = 0$). Now, if we demonstrate the

$$\int_{-\infty}^{\infty}\omega G^{\text{out}}(\mathbf{r},\mathbf{r}')d\omega = 2\pi i\delta(\mathbf{r}-\mathbf{r}'), \tag{5.70}$$

for Green's function, by using initial condition, we may simplify the proof of (5.59). Next, taking the inverse Fourier transform of both sides of (5.25), we get

$$p(\mathbf{r},t) = \frac{-i}{2\pi}\left(\int_{-\infty}^{\infty}\int_{V^{(m)}}\omega p_0^{(\text{m})}(\mathbf{r}')G_{ms}^{\text{out}}(\mathbf{r}',\mathbf{r})d\mathbf{r}'\right)e^{-i\omega t}d\omega. \tag{5.71}$$

When $t = 0$, for arbitrary m, the acoustic wave will be equal to the source function, i.e. $p(\mathbf{r}, 0) = p_0(\mathbf{r})$. Then we write

$$p_0(\mathbf{r}) = \frac{-i}{2\pi} \int_V p_0(\mathbf{r}') \left(\int_{-\infty}^{\infty} \omega G^{\text{out}}(\mathbf{r}, \mathbf{r}') d\omega \right) d\mathbf{r}' \tag{5.72}$$

where V includes the source. Since (5.72) holds for arbitrary $\mathbf{r}$ and the former integral is valid over $\mathbf{R}^3$, we may write it more generally as follows:

$$p_0(\mathbf{r}) = \frac{-i}{2\pi} \int_{\mathbf{R}^3} p_0(\mathbf{r}') \left(\int_{-\infty}^{\infty} \omega G^{\text{out}}(\mathbf{r}, \mathbf{r}') d\omega \right) d\mathbf{r}'. \tag{5.73}$$

So, we obtain the following equation for the Green's function.

$$\int_{-\infty}^{\infty} \omega G^{\text{out}}(\mathbf{r}, \mathbf{r}') d\omega = 2\pi i \delta(\mathbf{r} - \mathbf{r}'). \tag{5.74}$$

Using (5.74) and the relations (5.15) and (5.16), we can rewrite the integrals in (5.68) over the surface ;

$$\begin{aligned} K_m^{(1)}(\mathbf{r}, \mathbf{r}') = & -\frac{\rho_s}{\rho_m} \pi \delta(\mathbf{r} - \mathbf{r}') \\ & + \frac{\rho_s}{2\rho_m} \int_{-\infty}^{\infty} i\omega \int_{S_m} \frac{\partial \left(G_{mm}^{\text{out}}(\mathbf{r}', \mathbf{r_s}) G_{mm}^{\text{in}}(\mathbf{r}, \mathbf{r_s}) \right)}{\partial n_{s_m}} dS_m d\omega \\ & + \int_{-\infty}^{\infty} i\omega \sum_{k=1, k \neq m}^{N} \frac{\rho(k)}{2} \int_{S_k} \frac{\partial (G_{mk}^{\text{out}}(\mathbf{r}', \mathbf{r_s}) G_{mk}^{\text{in}}(\mathbf{r}, \mathbf{r_s}))}{\partial n_{s_k}} dS_k d\omega, \end{aligned} \tag{5.75}$$

with $k \neq m$. Since the planar boundaries of the layers are assumed to be parallel to the measurement plane S,

$$\frac{\partial}{\partial n_{s_k}} = \frac{\partial}{\partial z_k} \tag{5.76}$$

holds. So, we have

$$K_m^{(1)}(\mathbf{r},\mathbf{r}') = -\frac{\rho_s}{\rho_m}\pi\delta(\mathbf{r}-\mathbf{r}') + \frac{\rho_s}{2\rho_m}\int_{-\infty}^{\infty} i\omega \int_{S_m} \frac{\partial\left(G_{mm}^{\text{out}}(\mathbf{r}',\mathbf{r_s})G_{mm}^{\text{in}}(\mathbf{r},\mathbf{r_s})\right)}{\partial z_m} dS_m d\omega + \int_{-\infty}^{\infty} i\omega \sum_{k=1}^{N} \frac{\rho(k)}{2} \int_{S_k} \frac{\partial(G_{mk}^{\text{out}}(\mathbf{r}',\mathbf{r_s})G_{mk}^{\text{in}}(\mathbf{r},\mathbf{r_s}))}{\partial z_k} dS_k d\omega. \quad (5.77)$$

On the boundary surfaces, subject to $\mathbf{r_s} > \mathbf{r}$ and $\mathbf{r_s} > \mathbf{r}'$, the imaginary parts of the multiplication of the Green's functions in (5.75) are independent of z_s. Therefore the derivative of the imaginary part of $G_{mk}^{\text{out}}G_{mk}^{\text{in}}$ with respect to z_s, where $m = k$ and $m \neq k$, is zero. The real part of the integration of $G_{mk}^{\text{out}}G_{mk}^{\text{in}}$ over ω is taken from $-\infty$ to ∞ equals to zero because of the fact that the Green's functions are even functions respect to the temporal frequency (by the definition of k_z). Then,

$$K_m^{(1)}(\mathbf{r},\mathbf{r}') = -\frac{\rho_s}{\rho_m}\pi\delta(\mathbf{r}-\mathbf{r}'). \quad (5.78)$$

Now, $K^{(2)}(\mathbf{r},\mathbf{r}')$ includes the integration over ω of the multiplication of the Green's functions by ω which have different subscripts as follows:

$$K_m^{(2)}(\mathbf{r},\mathbf{r}') = \int_{-\infty}^{\infty} i\omega \int_S G_{ms}^{\text{out}}(\mathbf{r}',\mathbf{r_s})\nabla_s G_{ks}^{\text{in}}(\mathbf{r},\mathbf{r_s})\mathbf{n}dSd\omega, \quad (5.79)$$

$k \neq m$ and $m, k \leq N$. Using (5.58), we rewrite the above equation as

$$K_m^{(2)}(\mathbf{r},\mathbf{r}') = \int_{-\infty}^{\infty} i\omega \int_S \left[\nabla_s\left(G_{ms}^{\text{out}}(\mathbf{r}',\mathbf{r_s})\left(\nabla_s \sum_{k=1,k\neq m}^{N} \rho(k)G_{ks}^{\text{in}}(\mathbf{r},\mathbf{r_s})\right)\right) + \sum_{k=1,k\neq m}^{N}\left(\delta_{ks}G_{ks}^{\text{in}}(\mathbf{r},\mathbf{r_s})\delta(\mathbf{r}'-\mathbf{r_s}) - \delta_{ms}G_{ms}^{\text{out}}(\mathbf{r}',\mathbf{r_s})\delta(\mathbf{r}-\mathbf{r_s})\right)\right].\mathbf{n}dSd\omega. \quad (5.80)$$

From the definition of the Kronecker delta, the second part of (5.80) equals to zero. So, we write

$$K_m^{(2)}(\mathbf{r},\mathbf{r}') = \int_{-\infty}^{\infty} i\omega \int_S \left[\nabla_s \left(G_{ms}^{\text{out}}(\mathbf{r}',\mathbf{r_s}) \left(\nabla_s \sum_{k=1,k\neq m}^{N} \rho(k) G_{ks}^{\text{in}}(\mathbf{r},\mathbf{r_s}) \right) \right) \right] \mathbf{n} dS d\omega. \tag{5.81}$$

By using similar calculation and definition as (5.77), we see at once that $K^{(2)}(\mathbf{r},\mathbf{r}')$ is zero. In view of this fact, and substituting $K_m(\mathbf{r}',\mathbf{r})$ into (5.61), we obtain

$$q(\mathbf{r}) = p_0(\mathbf{r}).$$

Here $\mathbf{r}'$ and $\mathbf{r}$ are both in the mth layer. Then we derive, analytically, the inverse solution in the frequency domain for the multi-layer planar medium as follows:

$$q(\mathbf{r}) = \frac{1}{\pi}\frac{\rho_m}{\rho_s} \int_S \int_{-\infty}^{\infty} P(\mathbf{r_s},\omega) \frac{\partial G_{ms}^{\text{in}}(\mathbf{r},\mathbf{r_s})}{\partial n} d\omega dS, \quad \text{for} \quad \mathbf{r},\mathbf{r_s} \in \mathbb{R}^3 \tag{5.82}$$

Chapter 6

Explicit Expression Of The Green's Functions For Homogeneous and Two Layer Medium In Two Dimensional Cartesian Geometry

6.1 Green's Function For Homogeneous Medium (N = 1) In Two Dimensional Cartesian Coordinates

We solve the forward and the inverse problem for homogeneous medium in two dimensional Cartesian coordinates subject to radiation conditions and jump discontinuity. Homogeneous medium is shown in the following Fig.(6.2).

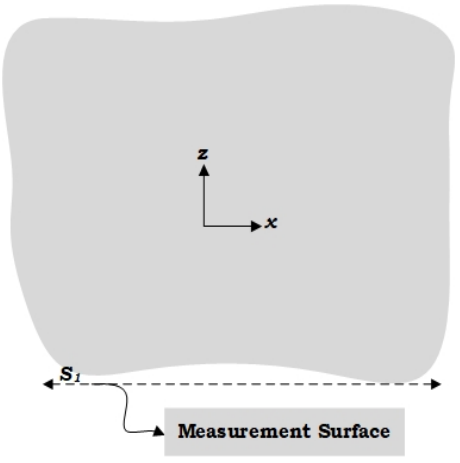

Figure 6.1: Homogenous medium.

Here, acoustic velocity and density of medium are same in medium. We assume that measurement surface is bottom of the medium with the source distribution

existing in all medium. Also, we assume that there is another line S_1' (parallel to S_1) at infinity and the combination of S_1' and S_1 encloses the source inside. For convenience, we define $S = S_1' + S_1$. We know from the equation (5.2) that the thermoacoustic wave equation is expressed as follows:

$$\left(\nabla^2 - \frac{1}{c^2}\frac{\partial^2}{\partial t^2}\right) p(\mathbf{r}, t) = -p_0(\mathbf{r})\frac{\partial \delta(t)}{\partial t} \tag{6.1}$$

where $\mathbf{r} = (x, z) \in \mathbb{R}^2$. In the forward problem we assume that $p_0(\mathbf{r})$ is known and find the wave function $p(\mathbf{r}, t)$ for all $\mathbf{r} \in \mathbb{R}^2$ and $t \in R$. In the inverse problem the acoustic wave function $p(\mathbf{r}, t)$ is known (by measurements) during a certain time interval on a surface S, and we try to determine the source function $p_0(\mathbf{r})$.

By using (5.59), we express the inverse solution of the thermoacoustic problem. Since the medium is homogeneous, $N = 1$, and the density rate equal to 1. Then inverse solution for homogeneous medium is as follows:

$$q(\mathbf{r}) = \frac{1}{\pi}\int_S \int_{-\infty}^{\infty} P(\mathbf{r_s}, \omega)\frac{G_{\mathrm{h}}^{\mathrm{in}}(\mathbf{r}', \mathbf{r_s})}{\partial \mathrm{n}} d\omega dS. \tag{6.2}$$

where S is the measurement surface (assumed that bottom of the medium), $\mathbf{r_s} = (x, z)$ and $\mathbf{r}' = (x', z')$ are measurement and source location, respectively. G_{h} denotes the homogeneous Green's function.

To solve the forward problem, subject to the given source function, we find the acoustic wave function $p(\mathbf{r}, t)$ for all $\mathbf{r} \in \mathbb{R}^2$ in frequency domain. By taking the Fourier transform of the equation (6.1), we obtain

$$\nabla^2 P + k^2 P = i\omega p_0(\mathbf{r}), \tag{6.3}$$

which is known as Helmholtz equation. Assuming $\mathbf{r} = (x, z)$ and $\mathbf{r}' = (x', z')$ are the measurement and the source locations respectively, we write the following equations by using homogeneous Green's functions.

$$\nabla^2 G_h(\mathbf{r}, \mathbf{r}') + k^2 G_h(\mathbf{r}, \mathbf{r}') = -\delta(\mathbf{r} - \mathbf{r}'). \tag{6.4}$$

where $k = \dfrac{\omega}{c}$ is the wave number and $\delta(\mathbf{r} - \mathbf{r}') = \delta(x - x')\delta(z - z')$ is the Dirac delta function. Outgoing Green's function also satisfies the following equation:

$$\nabla^2 G_h^{\text{out}}(\mathbf{r}, \mathbf{r}') + k^2 G_h^{\text{out}}(\mathbf{r}, \mathbf{r}') = -\delta(\mathbf{r} - \mathbf{r}'). \tag{6.5}$$

By using (5.25) with $N = 1$, we write the forward solution (acoustic wave function) using the superposition of the Green's function and the source function as follows:

$$P(\mathbf{r}, \omega) = -i\omega \int_{V_0} p_0(\mathbf{r}') G_h^{\text{out}}(\mathbf{r}, \mathbf{r}') d\mathbf{r}'. \tag{6.6}$$

Now, we obtain the explicit expression of the Green's function for homogeneous medium. When we take the spatial Fourier transform in the x direction of equation (6.5), we obtain

$$\int_{-\infty}^{\infty} (\nabla^2 G_h^{\text{out}} + k^2 G_h^{\text{out}}) \exp(-ik_x) dx = -\int_{-\infty}^{\infty} \delta(x - x')\delta(z - z') \exp(-ik_x x) dx \tag{6.7}$$

where $k = \dfrac{\omega}{c}$ is the wave vector, and k_x is the spatial frequency in the x direction. Now, we investigate the left hand side of the equation (6.7)

$$\begin{aligned}
&\int_{-\infty}^{\infty} \left(\frac{\partial G_h^{\text{out}}}{\partial x^2} + \frac{\partial G_h^{\text{out}}}{\partial y^2} + k_1^2 G_h^{\text{out}} \right) \exp(-ik_x x) dx \\
&= \underbrace{\int_{-\infty}^{\infty} \frac{\partial^2 G_h^{\text{out}}}{\partial x^2} \exp(-ik_x x) dx}_{(1a)} + \underbrace{\int_{-\infty}^{\infty} \frac{\partial^2 G_h^{\text{out}}}{\partial y^2} \exp(-ik_x x) dx}_{(2a)} \\
&\quad + \underbrace{k_1^2 \int_{-\infty}^{\infty} G_h^{\text{out}} \exp(-ik_x x) dx}_{(3a)}.
\end{aligned} \tag{6.8}$$

We take each part of (6.8) separately.

$$\begin{aligned}
(1a) &= \int_{-\infty}^{\infty} \frac{\partial^2 G_h^{\text{out}}}{\partial x^2} \exp(-ik_x x) dx \\
&= \lim_{a \to -\infty} \int_a^d \frac{\partial^2 G_h^{\text{out}}}{\partial x^2} \exp(-ik_x x) dx + \lim_{b \to \infty} \int_d^b \frac{\partial^2 G_h^{\text{out}}}{\partial x^2} \exp(-ik_x x) dx
\end{aligned} \tag{6.9}$$

where $d \in (-\infty, \infty)$.

If we apply the integration by parts to (6.9), we obtain

$$\begin{aligned}(1a) = &\lim_{a\to-\infty}\left(\frac{\partial G_h^{\text{out}}}{\partial x}\exp(-ik_x x)\right)\Big|_a^d + \lim_{b\to\infty}\left(\frac{\partial G_h^{\text{out}}}{\partial x}\exp(-ik_x x)\right)\Big|_d^b \\ &- \left(\lim_{a\to-\infty}(-ik_x)\int_a^d \frac{\partial G_h^{\text{out}}}{\partial x}\exp(-ik_x x)dx\right. \\ &\left. + \lim_{b\to\infty}(-ik_x)\int_d^b \frac{\partial G_h^{\text{out}}}{\partial x}\exp(-ik_x x)dx\right). \end{aligned} \tag{6.10}$$

Again, if we apply the integration by parts to the third and the fourth part of (6.10), we get

$$\begin{aligned}(1a) = &\lim_{a\to-\infty}\left(\frac{\partial G_h^{\text{out}}}{\partial x}\exp(-ik_x x)\right)\Big|_a^d + \lim_{b\to\infty}\left(\frac{\partial G_h^{\text{out}}}{\partial x}\exp(-ik_x x)\right)\Big|_d^b \\ &+ \left(\lim_{a\to-\infty}(ik_x)G_h^{\text{out}}\exp(-ik_x x)\right)\Big|_a^d + \left(\lim_{b\to\infty}(ik_x)G_h^{\text{out}}\exp(-ik_x x)\right)\Big|_d^b \\ &+ \lim_{a\to-\infty}\left(ik_x\int_a^d G_h^{\text{out}}\exp(-ik_x x)dx\right) + \lim_{b\to\infty}\left(ik_x\int_d^b G_h^{\text{out}}\exp(-ik_x x)dx\right) \\ = &\lim_{a\to-\infty}\left(\underbrace{\exp(-ik_x x)\left(\frac{\partial G_h^{\text{out}}}{\partial x} + ik_x G_h^{\text{out}}\right)\Big|_a^d}_{1AA}\right) \\ &+ \lim_{b\to\infty}\left(\underbrace{\exp(-ik_x x)\left(\frac{\partial G_h^{\text{out}}}{\partial x} + ik_x G_h^{\text{out}}\right)\Big|_d^b}_{1AB}\right) - k_x^2\hat{G}_h^{\text{out}} \end{aligned} \tag{6.11}$$

Subject to the radiation condition (5.7), the parts $(1AA)$ and $(1AB)$ goes to zero, as $a \to -\infty$ and $b \to \infty$. So,

$$(1a) = -k_x^2\hat{G}_h^{\text{out}} \tag{6.12}$$

We also calculate $(2a)$ and $(3a)$ of equation (6.8) as follow:

$$\begin{aligned}(2a) &= \int_{-\infty}^{\infty} \frac{\partial^2 G_h^{\text{out}}}{\partial z^2} \exp(-ik_x x)dx = \int_{-\infty}^{\infty} \frac{\partial^2}{\partial z^2} G_h^{\text{out}} \exp(-ik_x x)dx \\ &= \frac{\partial^2}{\partial z^2}\hat{G}_h. \qquad (6.13)\\ (3a) &= k^2 \int_{-\infty}^{\infty} G_h^{\text{out}} \exp(-ik_x x)dx \\ &= k^2 \hat{G}_h. \qquad (6.14)\end{aligned}$$

Then, the left hand side of (6.8) will be equal to

$$\frac{\partial^2 \hat{G_h^{\text{out}}}}{\partial z^2} - k_x^2 \hat{G_h^{\text{out}}} + k^2 \hat{G}_h. \qquad (6.15)$$

We write the equation (6.7) as the following using (6.15):

$$\frac{\partial^2 \hat{G_h^{\text{out}}}}{\partial z^2} - k_x^2 \hat{G_h^{\text{out}}} + k^2 \hat{G_h^{\text{out}}} = -\exp(-ik_x x')\delta(z - z'). \qquad (6.16)$$

We define $k_x^2 - k^2 = k_z^2$. So, we can write the following equation.

$$\frac{\partial^2 \hat{G}_h^{\text{out}}}{\partial z^2} - k_z^2 \hat{G}_h^{\text{out}} = -\exp(-ik_x x')\delta(z - z') \qquad (6.17)$$

where k_z is given by

$$k_z = \begin{cases} \sqrt{k_x^2 - (\frac{\omega}{c})^2}, & |\ k_x\ | > |\ \frac{\omega}{c}\ | \\ -i\sqrt{(\frac{\omega}{c})^2 - k_x^2}, & |\ k_x\ | < |\ \frac{\omega}{c}\ | \end{cases}. \qquad (6.18)$$

When the $z \neq z'$, the differential equation (6.17) is reduced the homogeneous linear equation

$$\frac{\partial z^2 \hat{G}_h^{\text{out}}}{\partial y^2} - k_z^2 \hat{G}_h^{\text{out}} = 0. \qquad (6.19)$$

The solution of (6.19) is written as

$$\hat{G}_h^{\text{out}} = \begin{cases} C_1 e^{ik_z z} + C_2 e^{-ik_z z} & 0 < z' < z \\ C_3 e^{ik_z z} + C_4 e^{-ik_z z} & z < z' < 0 \end{cases} . \tag{6.20}$$

We have to calculate the coefficients C_i $(i = 1, 2, 3, 4)$ to express the Green's function for homogeneous medium. To calculate the coefficients, we use radiation condition and the jump discontinuity as follows:

1) As $z \to \infty$, the coefficient C_1 equals zero from the radiation condition.

2) Green's function is continuous at $y = y'$, so

$$\begin{aligned} C_1 e^{ik_z z'} + C_2 e^{-ik_z z'} &= C_3 e^{ik_z z'} + C_4 e^{-ik_z z'} \\ C_1 e^{ik_z z'} + C_2 e^{-ik_z z'} - C_3 e^{ik_z z'} - C_4 e^{-ik_z z'} &= 0. \end{aligned} \tag{6.21}$$

3) At $z = z'$, we write as the following equation by using (5.45)

$$\frac{\partial (C_1 e^{ik_z z} + C_2 e^{-ik_z z})}{\partial z} - \frac{\partial (C_3 e^{ik_z z} + C_4 e^{-ik_z z})}{\partial z} = -e^{-ik_x x'}. \tag{6.22}$$

and we get

$$ik_z C_1 e^{ik_z z'} - ik_z C_2 e^{-ik_z z'} - ik_z C_3 e^{ik_z z'} + ik_z C_4 e^{-ik_z z'}. \tag{6.23}$$

4) As $z \to -\infty$, the coefficient C_4 is 0 because of the radiation conditions.

Subject to the above conditions, we write (6.17) as the following system of linear equations:

$$\begin{bmatrix} 1 & 0 & 0 & 0 \\ e^{ik_z z'} & e^{-ik_z z'} & -e^{ik_z z'} & -e^{-ik_z z'} \\ ik_z e^{ik_z z'} & -ik_z e^{-ik_z z'} & -ik_z e^{ik_z z'} & ik_z e^{-ik_z z'} \\ 0 & 0 & 0 & 1 \end{bmatrix} \times \begin{bmatrix} C_1 \\ C_2 \\ C_3 \\ C_4 \end{bmatrix} = \begin{bmatrix} 0 \\ 0 \\ -e^{-ik_x x'} \\ 0 \end{bmatrix} . \tag{6.24}$$

We can use the Cramer's rule to calculate the coefficients of the Green's function. Now we write the following determinant which is called A_h:

$$A_h = \begin{vmatrix} 1 & 0 & 0 & 0 \\ e^{ik_z z'} & e^{-ik_z z'} & -e^{ik_z z'} & -e^{-ik_z z'} \\ ik_z e^{ik_z z'} & -ik_z e^{-ik_z z'} & -ik_z e^{ik_z z'} & ik_z e^{-ik_z z'} \\ 0 & 0 & 0 & 1 \end{vmatrix}. \tag{6.25}$$

Since the measurement surface is the bottom of the medium according to our assumption, we must only find C_3 and to this end $\triangle_3$:

$$\triangle_3 = \begin{vmatrix} 1 & 0 & 0 & 0 \\ e^{ik_z z'} & e^{-ik_z z'} & 0 & -e^{-ik_z z'} \\ ik_z e^{ik_z z'} & -ik_z e^{-ik_z z'} & -e^{-ik_x x'} & ik_z e^{-ik_z z'} \\ 0 & 0 & 0 & 1 \end{vmatrix}, \tag{6.26}$$

and we write

$$C_3 = \frac{\triangle_3}{A_h} = \frac{e^{-ik_x x' e^{-ik_z z'}}}{2ik_z} \tag{6.27}$$

using Cramer's rule.

If we use (6.20) and then take the inverse Fourier transform, we obtain the outgoing Green's function for the homogeneous medium as

$$G_h^{\text{out}} = \frac{1}{2\pi} \int_{-\infty}^{\infty} \frac{e^{-ik_z|z-z'|} e^{ik_x(x-x')}}{2ik_z} dk_x. \tag{6.28}$$

6.2 Green's Functions For Two-Layer (N=2) Medium In Two Dimensional Cartesian Coordinates

We solve the forward problem and the inverse problem assuming the source distribution is in all layers for two-layer medium in two dimensional Cartesian coordinates subject to the continuity conditions on the boundary surface, jump

discontinuity at the source location and the radiation conditions at infinity. Two layer medium geometry is shown in Fig. (6.2)

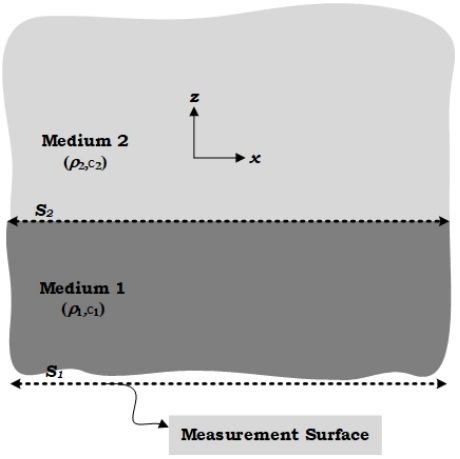

Figure 6.2: Two-layered medium.

where $z = l$ is the layer boundary coordinates, ρ_1 and ρ_2 are densities, and c_1 and c_2 are the acoustic velocities of the medium 1 and medium 2, respectively.

Using (5.82), inverse solution of the thermoacoustic problem for two layers ($N = 2$) in two dimensions is expressed as the following Case 1 and Case 2.

Case 1: The source is in the medium 1 i.e. $m = 1$:

$$q(\mathbf{r}') = \frac{1}{\pi}\frac{\rho_1}{\rho_s}\int_S\int_{-\infty}^{\infty} P(\mathbf{r},\omega)\frac{\partial G_{1s}^{\text{in}}(\mathbf{r},\mathbf{r}')}{\partial \mathbf{n}} d\omega dS. \tag{6.29}$$

Case 2: The source is in the medium 2, i.e. $m = 2$:

$$q(\mathbf{r}') = \frac{1}{\pi}\frac{\rho_2}{\rho_s}\int_S\int_{-\infty}^{\infty} P(\mathbf{r},\omega)\frac{\partial G_{2s}^{\text{in}}(\mathbf{r},\mathbf{r}')}{\partial \mathbf{n}} d\omega dS. \tag{6.30}$$

Using (5.25), the forward solution of the thermoacoustic problem for two layers ($N = 2$) in two dimensions is expressed as

$$\begin{aligned} P(\mathbf{r},\omega) &= -i\omega \sum_{m=1}^{2} \int_{V^{(\mathrm{m})}} p_0^{(\mathrm{m})}(\mathbf{r}')G_{ms}^{\mathrm{out}}(\mathbf{r}',\mathbf{r})d\mathbf{r}' \\ &= -i\omega \int_{V^{(1)}} p_0^{(1)}(\mathbf{r}')G_{1s}^{\mathrm{out}}(\mathbf{r}',\mathbf{r})d\mathbf{r}' + (-i\omega) \int_{V^{(2)}} p_0^{(2)}(\mathbf{r}')G_{2s}^{\mathrm{out}}(\mathbf{r}',\mathbf{r})d\mathbf{r}'. \end{aligned} \tag{6.31}$$

Here, $\mathbf{r} = (x, z)$ and $\mathbf{r}' = (x', z')$ are measurement and source coordinates, respectively. $V^{(1)}$ and $V^{(2)}$ denote the volumes which enclose the source $p_0^{(1)}$ in medium 1 and the source $p_0^{(2)}$ in medium 2, respectively. And we assume that S is the measurement surface (bottom of the layers, and parallel to the x axis) as we show in Fig.(6.2) and assume that there is another line S_1' (parallel to S_1) at infinity and the combination of S_1' and S_1 encloses the source inside. For convenience, we define $S = S_1' + S_1$.

To solve the inverse solution, we need to calculate $G_{1s}^{\mathrm{out}}(\mathbf{r}',\mathbf{r})$ and $G_{2s}^{\mathrm{out}}(\mathbf{r}',\mathbf{r})$, as well as the conjugates of these functions.

i) Firstly, we suppose that the source is in the first layer. For two layer medium in two dimensional geometry, we write the following wave equation by using (5.2):

$$\left(\nabla^2 - \frac{1}{c^2}\frac{\partial^2}{\partial t^2}\right) p(\mathbf{r},t) = -p_0(\mathbf{r})\frac{\partial \delta(t)}{\partial t}, \tag{6.32}$$

where $\mathbf{r} = (x, z)$. If we take the Time Fourier transform of (6.32), we obtain the Helmholtz equation as follows:

$$\nabla^2 P + k_1^2 P = i\omega p_0(\mathbf{r}), \tag{6.33}$$

where k_1 is the wave number in the first layer. We can write the following equation by using Green's function from (5.17):

$$\nabla^2 G_{1s}^{\text{out}}(\mathbf{r}^{'}, \mathbf{r}) + k_1^2 G_{1s}^{\text{out}}(\mathbf{r}^{'}, \mathbf{r}) = -\delta^{(1)}(\mathbf{r} - \mathbf{r}^{'}). \tag{6.34}$$

where $\mathbf{r}' = (x', z')$ and $\mathbf{r} = (x, z)$ are the source and the measurement locations respectively. When we take the spatial Fourier transform in the x direction of (6.34), we get

$$\begin{aligned} &\int_{-\infty}^{\infty} (\nabla^2 G_{1s}^{\text{out}} + k_1^2 G_{1s}^{\text{out}}) \exp(-ik_x x) dx \\ &= -\int_{-\infty}^{\infty} \delta^{(1)}(x - x') \delta^{(1)}(z - z') \exp(-ik_x x) dx. \end{aligned} \tag{6.35}$$

Here $k_1 = \dfrac{\omega}{c_1}$ is wave vector, and k_x is the spatial frequency.

Let's examine the left hand side of (6.35):

$$\begin{aligned} &\int_{-\infty}^{\infty} \left(\frac{\partial G_{1s}^{\text{out}}}{\partial x^2} + \frac{\partial G_{1s}^{\text{out}}}{\partial z^2} + k_1^2 G_{1s}^{\text{out}} \right) \exp(-ik_x x) dx \\ &= \underbrace{\int_{-\infty}^{\infty} \frac{\partial^2 G_{1s}^{\text{out}}}{\partial x^2} \exp(-ik_x x) dx}_{(1b)} + \underbrace{\int_{-\infty}^{\infty} \frac{\partial^2 G_{1s}^{\text{out}}}{\partial z^2} \exp(-ik_x x) dx}_{(2b)} \\ &\quad + \underbrace{k_1^2 \int_{-\infty}^{\infty} G_{1s}^{\text{out}} \exp(-ik_x x) dx}_{(3b)}. \end{aligned} \tag{6.36}$$

We also examine each part of (6.36), separately.

$$(1b) = \int_{-\infty}^{\infty} \frac{\partial^2 G_{1s}^{\text{out}}}{\partial x^2} \exp(-ik_x x) dx. \tag{6.37}$$

Applying the integration by parts to (6.37), we obtain

$$(1b) = \lim_{a\to-\infty}\left(\frac{\partial G_{1s}^{\text{out}}}{\partial x}\exp(-ik_x x)\Big|_a^d\right) + \lim_{b\to\infty}\left(\frac{\partial G_{1s}^{\text{out}}}{\partial x}\exp(-ik_x x)\Big|_d^b\right) - (-ik_x)\int_{-\infty}^{\infty}\frac{\partial G_{1s}^{\text{out}}}{\partial x}\exp(-ik_x x)dx. \tag{6.38}$$

Next, if we apply the integration by parts to (6.38) oncemore, to the second part of $(1b)$, we get

$$\begin{aligned}(1b) &= \lim_{a\to-\infty}\left(\frac{\partial G_{1s}^{\text{out}}}{\partial x}\exp(-ik_x x)\ \Big|_a^d\right) + \lim_{b\to\infty}\left(\frac{\partial G_{1s}^{\text{out}}}{\partial x}\exp(-ik_x x)\Big|_d^b\right)\\ &\quad + \lim_{a\to-\infty}\left(ik_x\left(G_{1s}^{\text{out}}\exp(-ik_x x)\Big|_a^d\right)\right) + \lim_{b\to\infty}\left(ik_x\left(G_{1s}^{\text{out}}\exp(-ik_x x)\Big|_d^b\right)\right)\\ &\quad + \lim_{a\to-\infty}\left(ik_x\int_a^d G_{1s}^{\text{out}}\exp(-ik_x x)dx\right) + \lim_{b\to\infty}\left(ik_x\int_d^b G_{1s}^{\text{out}}\exp(-ik_x x)dx\right)\\ &= \lim_{a\to-\infty}\left(\exp(-ik_x x)\underbrace{\left(\frac{\partial G_{1s}^{\text{out}}}{\partial x}+ik_x G_{1s}^{\text{out}}\right)\Big|_a^d}_{(1BA)}\right)\\ &\quad + \lim_{b\to\infty}\left(\exp(-ik_x x)\underbrace{\left(\frac{\partial G_{1s}^{\text{out}}}{\partial x}+ik_x G_{1s}^{\text{out}}\right)\Big|_d^b}_{(1BB)}\right) - k_x^2\hat{G}_{1s}^{\text{out}}.\end{aligned} \tag{6.39}$$

Subject to the radiation condition (5.7), the part $(1BA)$ and $(1BB)$ vanish as $a\to-\infty$ and $b\to\infty$, respectively. So,

$$(1b) = -k_x^2\hat{G}_{1s}^{\text{out}}. \tag{6.40}$$

We also calculate the parts $(2b)$ and $(3b)$ of the equation (6.36) as

$$\begin{aligned}(2b) &= \int_{-\infty}^{\infty} \frac{\partial^2 G_{1s}^{\text{out}}}{\partial z^2} \exp(-ik_x x)dx = \int_{-\infty}^{\infty} \frac{\partial^2}{\partial z^2} G_{1s}^{\text{out}} \exp(-ik_x x)dx \\ &= \frac{\partial^2}{\partial z^2} \hat{G}_{1s}^{\text{out}}. \qquad (6.41) \\ (3b) &= k_1^2 \int_{-\infty}^{\infty} G_{1s}^{\text{out}} \exp(-ik_x x)dx \\ &= k_1^2 \hat{G}_{1s}^{\text{out}}. \qquad (6.42)\end{aligned}$$

Then, the left hand side of (6.35) equals to

$$\frac{\partial^2 \hat{G_{1s}^{\text{out}}}}{\partial z^2} - k_x^2 \hat{G_{1s}^{\text{out}}} + k_1^2 \hat{G}^{\text{out}}. \qquad (6.43)$$

By using (6.43), we write the Fourier transform of (6.35) as follows:

$$\frac{\partial^2 \hat{G_{1s}^{\text{out}}}}{\partial z^2} - k_x^2 \hat{G_{1s}^{\text{out}}} + k_1^2 \hat{G_{1s}^{\text{out}}} = -\exp(-ik_x x')\delta(z - z'). \qquad (6.44)$$

Let us call $k_x^2 - k_1^2 = k_{z1}^2$. So, we can write the following equation.

$$\frac{\partial^2 \hat{G}_{1s}^{\text{out}}}{\partial z^2} - k_{z1}^2 \hat{G}_{1s}^{\text{out}} = -\exp(-ik_x x')\delta(z - z'). \qquad (6.45)$$

where k_{z1} is defined as follows:

$$k_{z1} = \begin{cases} \sqrt{k_x^2 - (\frac{\omega}{c_1})^2}, & |\ k_x\ | > |\ \frac{\omega}{c_1}\ | \\ -i\sqrt{(\frac{\omega}{c_1})^2 - k_x^2}, & |\ k_x\ | < |\ \frac{\omega}{c_1}\ | \end{cases}. \qquad (6.46)$$

Excluding the case $z = z'$, (6.45) is reduced to the homogeneous linear differential equation

$$\frac{\partial^2 \hat{G}_{1s}^{\text{out}}}{\partial z^2} - k_{z1}^2 \hat{G}_{1s}^{\text{out}} = 0. \qquad (6.47)$$

Using (5.50), we represent the solution of (6.47) by

$$\hat{G}_1^{\text{out}} = \begin{cases} C_1 e^{k_{z2}z} + C_2 e^{-k_{z2}z} & 0 < z \\ C_3 e^{k_{z1}z} + C_4 e^{-k_{z1}z} & z' < z < 0 \\ C_5 e^{k_{z1}z} + C_6 e^{-k_{z1}z} & z < z' \end{cases} . \tag{6.48}$$

Here, $\hat{G}_1^{\text{out}}$ stands for the wave propagation when the source is in the medium 1, and

$$k_{z2} = \begin{cases} \sqrt{k_x^2 - (\frac{\omega}{c_2})^2}, & \mid k_x \mid > \mid \frac{\omega}{c_2} \mid \\ -i\sqrt{(\frac{\omega}{c_2})^2 - k_x^2}, & \mid k_x \mid < \mid \frac{\omega}{c_2} \mid \end{cases} . \tag{6.49}$$

We need to find the pressure wave on the surface for finding the measured pressure. Therefore we must calculate the coefficient C_5 for $\hat{G}_{1s}^{\text{out}}$. Here the first index of $\hat{G}_{1s}^{\text{out}}$ indicates the medium which includes the source and the second index of the Green's function indicates the measurement surface. After we calculate the coefficient C_5, we take the inverse Fourier transform of $\hat{G}_{1s}^{\text{out}}$ to be able to write the explicit expression of G_{1s}^{out}. The Green's function satisfies continuity conditions on the layer boundary, jump discontinuity and continuity at the source location and the radiation condition as z goes to $-\infty$ and z goes to ∞. Now, let us write these conditions provided by the Green's function step by step.

1) Using radiation condition as $z \to \infty$, we say that $C_1 = 0$.

2) From the continuity condition on the layer boundary at $z = l$ we get

$$C_1 e^{k_{z2}l} + C_2 e^{-k_{z2}l} = C_3 e^{k_{z1}l} + C_4 e^{-k_{z1}l}. \tag{6.50}$$

3) Also, we write the following equation from the continuity condition on the layer boundary at $y = l$,

$$\frac{1}{\rho_1}\frac{\partial(C_1 e^{k_{z2}z} + C_2 e^{-k_{z2}z})}{\partial z} = \frac{1}{\rho_2}\frac{\partial(C_3 e^{k_{z1}z} + C_4 e^{-k_{z1}z})}{\partial z}$$

$$\frac{\rho_2}{\rho_1}k_{z2}C_1 e^{k_{z2}l} - \frac{\rho_2}{\rho_1}k_{z2}C_2 e^{-k_{z2}l} = k_{z1}C_3 e^{k_{z1}l} - k_{z1}C_4 e^{-k_{z1}l}. \tag{6.51}$$

4) Green's function is continuous at $z = z'$, so we write

$$C_3 e^{k_{z1}z'} + C_4 e^{-k_{z1}z'} - C_5 e^{k_{z1}z'} - C_6 e^{-k_{z1}z'} = 0. \tag{6.52}$$

5) We write the following equation at $y = y'$ using the jump discontinuity (5.45):

$$\frac{\partial(C_3 e^{k_{z1}z} + C_4 e^{-k_{z1}z})}{\partial z} - \frac{\partial(C_5 e^{k_{z1}z} + C_6 e^{-k_{z1}z})}{\partial z} = -e^{-ik_x x'}. \tag{6.53}$$

If we take the partial derivatives and we write z' instead of z in (6.53), we obtain

$$k_{y1}e^{k_{z1}z'}C_3 - k_{z1}e^{-k_{z1}z'}C_4 - k_{z1}e^{k_{z1}z'}C_5 + k_{z1}e^{-k_{z1}z'}C_6 = -e^{-ik_x x'}. \tag{6.54}$$

6) We see that C_6 vanishes using the radiation condition as $z \to -\infty$.

Using (6.50), (6.51), (6.52), (6.54), and the radiation conditions, we write the following system of linear equations:

$$\begin{bmatrix} 1 & 0 & 0 & 0 & 0 & 0 \\ e^{k_{z2}l} & e^{-k_{z2}l} & -e^{k_{z1}l} & -e^{-k_{z1}l} & 0 & 0 \\ \frac{\rho_2}{\rho_1}k_{z2}e^{k_{z2}l} & -\frac{\rho_2}{\rho_1}k_{z2}e^{-k_{z2}l} & -k_{z1}e^{k_{z1}l} & k_{z1}e^{-k_{z1}l} & 0 & 0 \\ 0 & 0 & e^{k_{z1}z'} & e^{-k_{z1}z'} & -e^{k_{z1}z'} & -e^{-k_{z1}z'} \\ 0 & 0 & k_{z1}e^{k_{z1}z'} & -k_{z1}e^{-k_{z1}z'} & -k_{z1}e^{k_{z1}z'} & k_{z1}e^{-k_{z1}z'} \\ 0 & 0 & 0 & 0 & 0 & 1 \end{bmatrix}$$

$$\times \begin{bmatrix} C_1 \\ C_2 \\ C_3 \\ C_4 \\ C_5 \\ C_6 \end{bmatrix} = \begin{bmatrix} 0 \\ 0 \\ 0 \\ 0 \\ -e^{-ik_x x'} \\ 0 \end{bmatrix}. \tag{6.55}$$

The coefficient C_5 is calculated by using the Cramer's Rule. Let us call

A as

$$\begin{bmatrix} 1 & 0 & 0 & 0 & 0 & 0 \\ e^{k_{z2}l} & e^{-k_{z2}l} & -e^{k_{z1}l} & -e^{-k_{z1}l} & 0 & 0 \\ \frac{\rho_2}{\rho_1}k_{z2}e^{k_{z2}l} & -\frac{\rho_2}{\rho_1}k_{z2}e^{-k_{z2}l} & -k_{z1}e^{k_{z1}l} & k_{z1}e^{-k_{z1}l} & 0 & 0 \\ 0 & 0 & e^{k_{z1}z'} & e^{-k_{z1}z'} & -e^{k_{z1}z'} & -e^{-k_{z1}z'} \\ 0 & 0 & k_{z1}e^{k_{z1}z'} & -k_{z1}e^{-k_{z1}z'} & -k_{z1}e^{k_{z1}z'} & k_{z1}e^{-k_{z1}z'} \\ 0 & 0 & 0 & 0 & 0 & 1 \end{bmatrix}, \tag{6.56}$$

C as

$$\begin{bmatrix} C_1 \\ C_2 \\ C_3 \\ C_4 \\ C_5 \\ C_6 \end{bmatrix}, \tag{6.57}$$

B as

$$\begin{bmatrix} 0 \\ 0 \\ 0 \\ 0 \\ -e^{-ik_x x'} \\ 0 \end{bmatrix}. \tag{6.58}$$

and finally, Δ_5 as

$$\begin{bmatrix} 1 & 0 & 0 & 0 & 0 & 0 \\ e^{k_{z2}l} & e^{-k_{z2}l} & -e^{k_{z1}l} & -e^{-k_{z1}l} & 0 & 0 \\ \frac{\rho_2}{\rho_1}k_{z2}e^{k_{z2}l} & -\frac{\rho_2}{\rho_1}k_{z2}e^{-k_{z2}l} & -k_{z1}e^{k_{z1}l} & k_{z1}e^{-k_{z1}l} & 0 & 0 \\ 0 & 0 & e^{k_{z1}z'} & e^{-k_{z1}z'} & 0 & -e^{-k_{z1}z'} \\ 0 & 0 & k_{z1}e^{k_{z1}z'} & -k_{z1}e^{-k_{z1}z'} & -e^{-ik_x x'} & k_{z1}e^{-k_{z1}z'} \\ 0 & 0 & 0 & 0 & 0 & 1 \end{bmatrix}. \tag{6.59}$$

Using Cramer's Rule, we write $C_5 = \dfrac{\mid \Delta_5 \mid}{\mid A \mid}$. At first, we calculate $\mid A \mid$ which is

$$\begin{vmatrix} 1 & 0 & 0 & 0 & 0 & 0 \\ e^{k_{z2}l} & e^{-k_{z2}l} & -e^{k_{z1}l} & -e^{-k_{z1}l} & 0 & 0 \\ \frac{\rho_2}{\rho_1}k_{z2}e^{k_{z2}l} & -\frac{\rho_2}{\rho_1}k_{z2}e^{-k_{z2}l} & -k_{z1}e^{k_{z1}l} & k_{z1}e^{-k_{z1}l} & 0 & 0 \\ 0 & 0 & e^{k_{z1}z'} & e^{-k_{z1}z'} & -e^{k_{z1}z'} & -e^{-k_{z1}z'} \\ 0 & 0 & k_{z1}e^{k_{z1}z'} & -k_{z1}e^{-k_{z1}z'} & -k_{z1}e^{k_{z1}z'} & k_{z1}e^{-k_{z1}z'} \\ 0 & 0 & 0 & 0 & 0 & 1 \end{vmatrix}. \tag{6.60}$$

If we add the third and the fourth columns to the fifth and sixth columns in (6.60), we obtain the following determinant.

$$\begin{vmatrix} 1 & 0 & 0 & 0 & 0 & 0 \\ e^{k_{z2}l} & e^{-k_{z2}l} & -e^{k_{z1}l} & -e^{-k_{z1}l} & -e^{k_{z1}l} & -e^{-k_{z1}l} \\ \frac{\rho_2}{\rho_1}k_{z2}e^{k_{z2}l} & -\frac{\rho_2}{\rho_1}k_{z2}e^{-k_{z2}l} & -k_{z1}e^{k_{z1}l} & k_{z1}e^{-k_{z1}l} & -k_{z1}e^{k_{z1}l} & k_{z1}e^{-k_{z1}l} \\ 0 & 0 & e^{k_{z1}z'} & e^{-k_{z1}z'} & 0 & 0 \\ 0 & 0 & k_{z1}e^{k_{z1}z'} & -k_{z1}e^{-k_{z1}z'} & 0 & 0 \\ 0 & 0 & 0 & 0 & 0 & 1 \end{vmatrix}. \quad (6.61)$$

Using the cofactor expansion along the third row and then the fourth column in (6.61), we obtain

$$\begin{aligned} & e^{k_{z1}z'} \begin{vmatrix} e^{-k_{z2}l} & -e^{-k_{z1}l} & -e^{k_{z1}l} \\ -\frac{\rho_2}{\rho_1}k_{z2}e^{-k_{z2}l} & k_{z1}e^{-k_{z1}l} & -k_{z1}e^{k_{z1}l} \\ 0 & -k_{z1}e^{k_{z1}z'} & 0 \end{vmatrix} \\ & - e^{-k_{z1}z'} \begin{vmatrix} e^{-k_{z2}l} & -e^{k_{z1}l} & -e^{k_{z1}l} \\ -\frac{\rho_2}{\rho_1}k_{z2}e^{-k_{z2}l} & -k_{z1}e^{k_{z1}l} & -k_{z1}e^{k_{z1}l} \\ 0 & k_{z1}e^{k_{z1}z'} & 0 \end{vmatrix} \quad (6.62) \\ & = k_{z1} \begin{vmatrix} e^{-k_{z2}l} & -e^{-k_{z1}l} \\ -\frac{\rho_2}{\rho_1}k_{z2}e^{-k_{z2}l} & -k_{z1}e^{k_{z1}l} \end{vmatrix} \\ & + k_{z1} \begin{vmatrix} e^{-k_{z2}l} & -e^{k_{z1}l} \\ -\frac{\rho_2}{\rho_1}k_{z2}e^{-k_{z2}l} & -k_{z1}e^{k_{z1}l} \end{vmatrix} \\ & = 2k_{z1}\left(-k_{z1}e^{l(k_{z1}-k_{z2})} - \frac{\rho_2}{\rho_1}k_{z2}e^{-l(k_{z1}+k_{z2})}\right) \quad (6.63) \end{aligned}$$

Then,

$$| A | = -2k_{z1}\left(k_{z1}e^{l(k_{z1}-k_{z2})} + \frac{\rho_2}{\rho_1}k_{z2}e^{-l(k_{z1}+k_{z2})}\right). \quad (6.64)$$

We must also calculate $\mid \Delta_5 \mid$ which is

$$\begin{vmatrix} 1 & 0 & 0 & 0 & 0 & 0 \\ e^{k_{z2}l} & e^{-k_{z2}l} & -e^{k_{z1}l} & -e^{-k_{z1}l} & 0 & 0 \\ \frac{\rho_2}{\rho_1}k_{z2}e^{k_{z2}l} & -\frac{\rho_2}{\rho_1}k_{z2}e^{-k_{z2}l} & -k_{z1}e^{k_{z1}l} & k_{z1}e^{-k_{z1}l} & 0 & 0 \\ 0 & 0 & e^{k_{z1}z'} & e^{-k_{z1}z'} & 0 & -e^{-k_{z1}z'} \\ 0 & 0 & k_{z1}e^{k_{z1}z'} & -k_{z1}e^{-k_{z1}z'} & -e^{-ik_x x'} & k_{z1}e^{-k_{z1}z'} \\ 0 & 0 & 0 & 0 & 0 & 1 \end{vmatrix}. \quad (6.65)$$

Using the cofactor expansion along the fifth column, we get

$$-e^{-ik_x x'} \begin{vmatrix} 1 & 0 & 0 & 0 & 0 \\ e^{k_{z2}l} & e^{-k_{z2}l} & -e^{k_{z1}l} & -e^{-k_{z1}l} & 0 \\ \frac{\rho_2}{\rho_1}k_{z2}e^{k_{z2}l} & -\frac{\rho_2}{\rho_1}k_{z2}e^{-k_{z2}l} & -k_{z1}e^{k_{z1}l} & k_{z1}e^{-k_{z1}l} & 0 \\ 0 & 0 & e^{k_{z1}z'} & e^{-k_{z1}z'} & -e^{-k_{z1}z'} \\ 0 & 0 & 0 & 0 & 1 \end{vmatrix},$$

and along the second column

$$-e^{-ik_x x'}e^{-k_{z2}l} \begin{vmatrix} -k_{z1}e^{k_{z1}l} & k_{z1}e^{-k_{z1}l} & 0 \\ e^{k_{z1}z'} & e^{-k_{z1}z'} & -e^{-k_{z1}z'} \\ 0 & 0 & 1 \end{vmatrix}$$

$$-e^{-ik_x x'}\frac{\rho_2}{\rho_1}k_{z2}e^{-k_{z2}l} \begin{vmatrix} -e^{k_{z1}l} & -e^{-k_{z1}l} & 0 \\ e^{k_{z1}z'} & e^{-k_{z1}z'} & -e^{-k_{y1}z'} \\ 0 & 0 & 1 \end{vmatrix}$$

$$= e^{-ik_x x'}k_{z1}\left(e^{-k_{z1}z'}e^{l(k_{z1}-k_{z2})} + e^{k_{z1}z'}e^{-l(k_{z1}+k_{z2})}\right)$$
$$+ e^{-ik_x x'}\frac{\rho_2}{\rho_1}k_{z2}\left(e^{-k_{z1}z'}e^{l(k_{z1}-k_{z2})} - e^{k_{z1}z'}e^{-l(k_{z1}+k_{z2})}\right). \quad (6.66)$$

So, we write

$$\begin{aligned} \mid \Delta_5 \mid = e^{-ik_x x'} e^{-k_{z1} z'} e^{l(k_{z1}-k_{z2})} \left(k_{z1} + \frac{\rho_2}{\rho_1} k_{z2} \right) \\ + e^{-ik_x x'} e^{k_{z1} z'} e^{-l(k_{z1}+k_{z2})} \left(k_{z1} - \frac{\rho_2}{\rho_1} k_{z2} \right). \end{aligned} \tag{6.67}$$

Using (6.64), (6.67) and the Cramer's Rule, we obtain

$$\begin{aligned} C_5 &= \frac{\mid \Delta_5 \mid}{\mid A \mid} \\ &= \frac{e^{-ik_x x'} e^{-k_{z1} z'} e^{l(k_{z1}-k_{z2})} \left(k_{z1} + \frac{\rho_2}{\rho_1} k_{z2} \right) + e^{-ik_x x'} e^{k_{z1} z'} e^{-l(k_{z1}+k_{z2})} \left(k_{z1} - \frac{\rho_2}{\rho_1} k_{z2} \right)}{-2k_{z1} \left(k_{z1} e^{l(k_{z1}-k_{z2})} + \frac{\rho_2}{\rho_1} k_{z2} e^{-l(k_{z1}+k_{z2})} \right)}. \end{aligned} \tag{6.68}$$

Then by using (6.68), we can write the explicit expression of $\hat{G}_{1s}^{\text{out}}$ as

$$e^{-ik_x x'} \left(\frac{e^{k_{z1}(z-z')} e^{l(k_{z1}-k_{z2})} \left(k_{z1} + \frac{\rho_2}{\rho_1} k_{z2} \right) + e^{k_{z1}(z+z')} e^{-l(k_{z1}+k_{z2})} \left(k_{z1} - \frac{\rho_2}{\rho_1} k_{z2} \right)}{-2k_{z1} \left(k_{z1} e^{l(k_{z1}-k_{z2})} + \frac{\rho_2}{\rho_1} k_{z2} e^{-l(k_{z1}+k_{z2})} \right)} \right). \tag{6.69}$$

If we take the spatial Fourier transformation of (6.69) in the x direction, we get the outgoing Green's function in the frequency domain:

$$\begin{aligned} G_{1s}^{\text{out}} = -\frac{1}{2\pi} \int_{-\infty}^{\infty} e^{ik_x(x-x')} \left(\frac{e^{k_{z1}(z-z')} e^{l(k_{z1}-k_{z2})} \left(k_{z1} + \frac{\rho_2}{\rho_1} k_{z2} \right)}{2k_{z1} \left(k_{z1} e^{l(k_{z1}-k_{z2})} + \frac{\rho_2}{\rho_1} k_{z2} e^{-l(k_{z1}+k_{z2})} \right)} \right. \\ \left. + \frac{e^{k_{z1}(z+z')} e^{-l(k_{z1}+k_{z2})} \left(k_{z1} - \frac{\rho_2}{\rho_1} k_{z2} \right)}{2k_{z1} \left(k_{z1} e^{l(k_{z1}-k_{z2})} + \frac{\rho_2}{\rho_1} k_{z2} e^{-l(k_{z1}+k_{z2})} \right)} \right) dk_x. \end{aligned} \tag{6.70}$$

ii) Secondly, we suppose that the source is in the second layer for two layer medium in two dimensional geometry. We shall state the explicit expression of G_{2s}^{out} which stands for the wave propagation from the source point to measurement surface subject to the continuity conditions on the layer boundaries, jump discontinuity and continuity at the source location and the radiation conditions. We represent $\hat{G}_2^{\text{out}}$ as

$$\hat{G}_2^{\text{out}} = \begin{cases} C_1 e^{k_{z2}z} + C_2 e^{-k_{z2}z} & 0 < z \\ C_3 e^{k_{z1}z} + C_4 e^{-k_{z1}z} & z' < z < 0 \\ C_5 e^{k_{z1}z} + C_6 e^{-k_{z1}z} & z < z' \end{cases} . \tag{6.71}$$

using similar calculations. Here $\hat{G}_2^{\text{out}}$ denotes the wave propagation when the source is in medium 2. We must find C_2 for the explicit expression of G_{2s}^{out}. Using (6.50), (6.51), (6.52), (6.54) and the radiation conditions, we obtain the following system of linear equations.

$$\begin{bmatrix} 1 & 0 & 0 & 0 & 0 & 0 \\ e^{k_{z2}l} & e^{-k_{z2}l} & -e^{k_{z1}l} & -e^{-k_{z1}l} & 0 & 0 \\ \frac{\rho_2}{\rho_1}k_{z2}e^{k_{z2}l} & -\frac{\rho_2}{\rho_1}k_{z2}e^{-k_{z2}l} & -k_{z1}e^{k_{z1}l} & k_{z1}e^{-k_{z1}l} & 0 & 0 \\ 0 & 0 & e^{k_{z1}z'} & e^{-k_{z1}z'} & -e^{k_{z1}z'} & -e^{-k_{z1}z'} \\ 0 & 0 & k_{z1}e^{k_{z1}z'} & -k_{z1}e^{-k_{z1}z'} & -k_{z1}e^{k_{z1}z'} & k_{z1}e^{-k_{z1}z'} \\ 0 & 0 & 0 & 0 & 0 & 1 \end{bmatrix}$$

$$\times \begin{bmatrix} C_1 \\ C_2 \\ C_3 \\ C_4 \\ C_5 \\ C_6 \end{bmatrix} = \begin{bmatrix} 0 \\ 0 \\ 0 \\ 0 \\ -e^{-ik_x x'} \\ 0 \end{bmatrix} . \tag{6.72}$$

Let us take

$$\Delta_2 = \begin{bmatrix} 1 & 0 & 0 & 0 & 0 & 0 \\ e^{k_{z2}l} & 0 & -e^{k_{z1}l} & -e^{-k_{z1}l} & 0 & 0 \\ \frac{\rho_2}{\rho_1}k_{z2}e^{k_{z2}l} & 0 & -k_{z1}e^{k_{z1}l} & k_{z1}e^{-k_{z1}l} & 0 & 0 \\ 0 & 0 & e^{k_{z1}z'} & e^{-k_{z1}z'} & -e^{k_{z1}z'} & -e^{-k_{z1}z'} \\ 0 & -e^{-ik_x x'} & k_{z1}e^{k_{z1}z'} & -k_{z1}e^{-k_{z1}z'} & -k_{z1}e^{k_{z1}z'} & k_{z1}e^{-k_{z1}z'} \\ 0 & 0 & 0 & 0 & 0 & 1 \end{bmatrix}. \tag{6.73}$$

Since $C_2 = \dfrac{\mid \Delta_2 \mid}{\mid A \mid}$, we must calculate the determinants of Δ_2 and A which was given by (6.56). We have,

$$\mid \Delta_2 \mid = \begin{vmatrix} 1 & 0 & 0 & 0 & 0 & 0 \\ e^{k_{z2}l} & 0 & -e^{k_{z1}l} & -e^{-k_{z1}l} & 0 & 0 \\ \frac{\rho_2}{\rho_1}k_{z2}e^{k_{z2}l} & 0 & -k_{z1}e^{k_{z1}l} & k_{z1}e^{-k_{z1}l} & 0 & 0 \\ 0 & 0 & e^{k_{z1}z'} & e^{-k_{z1}z'} & -e^{k_{z1}z'} & -e^{-k_{z1}z'} \\ 0 & -e^{-ik_x x'} & k_{z1}e^{k_{z1}z'} & -k_{z1}e^{-k_{z1}z'} & -k_{z1}e^{k_{z1}z'} & k_{z1}e^{-k_{z1}z'} \\ 0 & 0 & 0 & 0 & 0 & 1 \end{vmatrix}, \tag{6.74}$$

and using the cofactor expansion along the second column, (6.74) as

$$e^{-ik_x x'} \begin{vmatrix} 1 & 0 & 0 & 0 & 0 \\ e^{k_{z2}l} & -e^{k_{z1}l} & -e^{-k_{z1}l} & 0 & 0 \\ \frac{\rho_2}{\rho_1}k_{z2}e^{k_{z2}l} & -k_{z1}e^{k_{z1}l} & k_{z1}e^{-k_{z1}l} & 0 & 0 \\ 0 & e^{k_{z1}z'} & e^{-k_{z1}z'} & -e^{k_{z1}z'} & -e^{-k_{z1}z'} \\ 0 & 0 & 0 & 0 & 1 \end{vmatrix} \tag{6.75}$$

also using the cofactor expansion along the first and fifth column in (6.75), we get

$$
\begin{aligned}
&= e^{-ik_x x'} \begin{vmatrix} -e^{k_{z1}l} & -e^{-k_{z1}l} & 0 \\ -k_{z1}e^{k_{z1}l} & k_{z1}e^{-k_{z1}l} & 0 \\ e^{k_{z1}z'} & e^{-k_{z1}z'} & -e^{k_{z1}z'} \end{vmatrix} \\
&= -e^{-ik_x x'} e^{k_{z1}z'} \begin{vmatrix} -e^{k_{z1}l} & -e^{-k_{z1}l} \\ -k_{z1}e^{k_{z1}l} & k_{z1}e^{-k_{z1}l} \end{vmatrix} \\
&= e^{-ik_x x'} e^{k_{z1}z'} (2k_{z1}). \qquad (6.76)
\end{aligned}
$$

Next, using (6.64) and (6.76), we get

$$
\begin{aligned}
C_2 &= \frac{e^{-ik_x x'} e^{k_{z1}z'} (2k_{z1})}{-2k_{z1}\left(k_{z1}e^{l(k_{z1}-k_{z2})} + \frac{\rho_2}{\rho_1}k_{z2}e^{-l(k_{z1}+k_{z2})}\right)} \\
&= -\frac{e^{-ik_x x'} e^{k_{z1}z'}}{\left(k_{z1}e^{l(k_{z1}-k_{z2})} + \frac{\rho_2}{\rho_1}k_{z2}e^{-l(k_{z1}+k_{z2})}\right)}. \qquad (6.77)
\end{aligned}
$$

Then, it follows from (6.71), that we get

$$
\hat{G}_{2s}^{\text{out}} = -\frac{e^{-ik_x x'} e^{k_{z1}z'} e^{-k_{z2}z}}{\left(k_{z1}e^{l(k_{z1}-k_{z2})} + \frac{\rho_2}{\rho_1}k_{z2}e^{-l(k_{z1}+k_{z2})}\right)}, \qquad (6.78)
$$

whose inverse spatial Fourier transform of is

$$
G_{2s}^{\text{out}} = \int_{-\infty}^{\infty} \frac{-e^{k_{z1}z'} e^{-k_{z2}z} e^{ik_x(x-x')}}{\left(k_{z1}e^{l(k_{z1}-k_{z2})} + \frac{\rho_2}{\rho_1}k_{z2}e^{-l(k_{z1}+k_{z2})}\right)} dk_x. \qquad (6.79)
$$

By assuming the source distribution in all layer, to calculate the coefficients of Green's function for any N layer similar calculations calculations yield as using Cramer's Rule. The dimension of the matrix will increase as the number of the layers increase.

Chapter 7

Numerical Simulation

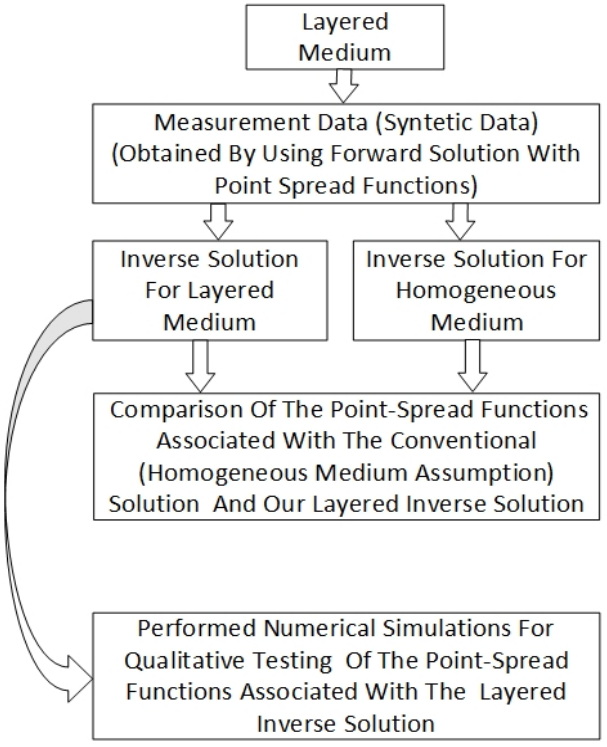

Figure 7.1: Schematic representation of the numerical simulation.

For qualitative testing and the comparison of the point-spread functions associated with the homogeneous and our layered solutions, we performed numerical simulations for two-layer (skin and fat) and three-layer (skin, fat and muscle) test phantom. In the numerical simulations, we considered a two-dimensional y-cross sectional geometry assuming that each layer extents to infinity in the third

dimension. We implemented our numerical simulations in Matlab running on workstation computers. The array of the acoustic detectors (transducers), which is relatively smaller than the medium sizes in lateral dimension, placed the outer of the first layer that is matched to the skin layer a distance of 5 mm away from the skin in the figures of simulations.

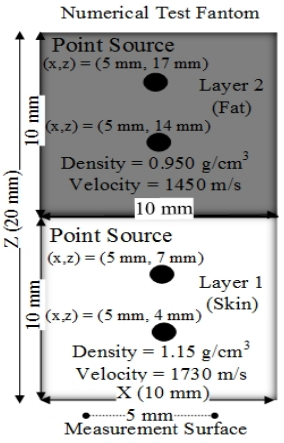

Figure 7.2: Numerical planar test fantom in two layer consists of two point sources in each layer.

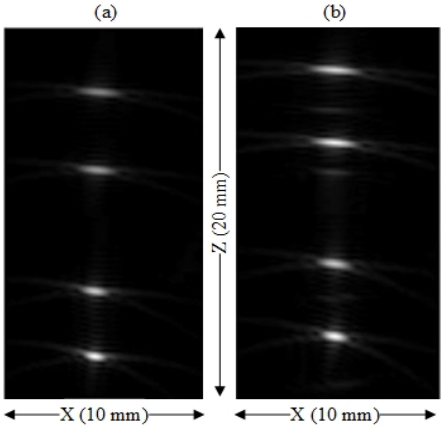

Figure 7.3: (a) Numerical simulation obtained by using the free space Green's function in the inversion algorithm (5.52) (result: incorrect source locations).(b) Numerical simulation obtained by using the layered Green's functions in the inversion algorithm (5.82) (result: correct source location) The display is in a linear scale.

We generated the measured data using the forward solution (5.25) with the layered outgoing Green's functions in the simulations. We take numerical planar test

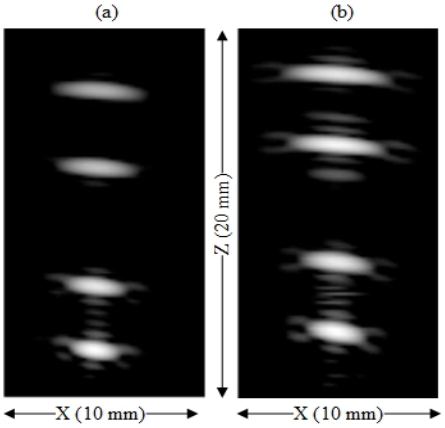

Figure 7.4: (a) Numerical simulation obtained by using the free space Green's function in the inversion algorithm (5.82) (with incorrect source locations).(b) Numerical simulation obtained by using the layered Green's functions in the inversion algorithm (5.82) (with correct source location) The display dynamic range is 20 dB (logarithmic scale).

phantom with two layers in Fig. 7.2 which has a size of 10 mm$\times$ 20 mm, consisting of two point sources in each layer for the skin and the fat layers which have 0.95 g/cm^3 and 1.15 g/cm^3 densities respectively, and the acoustic velocities are 1450 m/s and 1730 m/s, respectively. For comparison with the conventional solution and our layered solution, we used the free space Green's function where the ultrasound velocity and the density of medium were taken as the averages of the corresponding parameters of the layers in Fig.7.3 (a) and in Fig. 7.4 (a), also we used the layer Green's function where the velocity and the density of medium were taken as correct parameters of the layers in the inversion algorithm (5.82) in Fig. 7.3 (b) and in Fig. 7.4 (b) . In our computations, we have considered a 5 MHz temporal frequency band between 2.5 MHz and 7.5 MHz, which corresponds to a 5 MHz transducer with a 100% fractional bandwidth ($f_0 = 5$ MHz, FBW = 100). We sampled the temporal frequency band by $\Delta f = 70$ kHz steps in Fig.7.4, Fig. 7.5, and Fig. 7.6. In Fig. 7.2, the correct (x, z) coordinates of sources in Layer 1 are (5 mm, 4 mm) and (5 mm, 7 mm) respectively, and in Layer 2 are (5 mm, 14 mm) and (5 mm, 17 mm) respectively. For detection of the acoustic field, 32 point-like transducers with $\lambda_0/2$ an inter-element separation were placed at the bottom of the phantom. Transducer size is 5 mm. One can see that while

Fig. (7.3) (a) and Fig. (7.4) (a) have distorted and poor PSFs with incorrect locations (in z direction) of the point sources, $(x, z) = (5$ mm, 3 mm) and (5 mm, 5.5 mm) respectively, and the point sources's coordinates are $(x, z) = (5$ mm, 13 mm) and (5 mm, 16 mm), respectively in Layer 2 whereas Fig. 7.3 (b) and Fig. (7.4) (b) have exactly correct source locations.

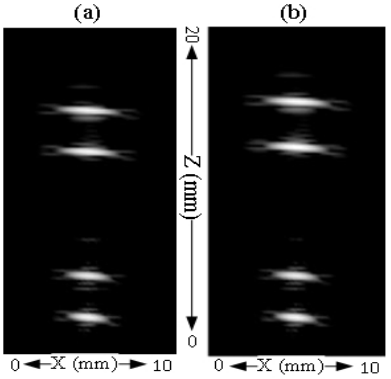

Figure 7.5: a)Image of the point spread function distribution with correct medium parameters by use of the inversion algorithm (5.82) (point source coordinates are $(x, z) =$(5 mm, 12.5 mm) and $(x, z) =$(5 mm,15 mm) respectively, in the first (upper) medium. (b) Image of the point spread function distribution when the speed of sound in the first (upper) layer is incorrectly estimated (10% incorrectly estimated). The point source coordinates are $(x, z) =$(5 mm, 13.12 mm) and $(x, z) =$(5 mm,16 mm) respectively, in (b). The display dynamic range is 20 dB (logarithmic scale).

In Fig. 7.5, the ultrasound velocity is assumed to be different from the actual value in the first layer only in the inversion algorithm (5.82). As the medium parameters may not be correctly known in practice, the robustness tests were performed to determine how well the algorithm performs with respect to the imprecise knowledge of various system parameters, e.g, ultrasound velocity. Especially, the ultrasound velocity assumed by the inversion algorithm is 1595 m/s (10 % larger than the actual value of 1450 m/s) and the display dynamic range is 20 dB. 32 point-like transducers with $\lambda_0/2$ an inter-element separation are placed at the bottom of the phantom ($f_0 = 5$ MHz, FBW = 100) for fat and skin. Transducer size is 5 mm. One can see that the location of reconstructed point source is incorrect in the z direction. Under the assumption of misestimation of ultrasound velocity c in any layer, the values set of k_z is erroneous. As a result error occurs in the estimated Fourier components of the source $p_0(\mathbf{r})$ which causes the shifting of the source location in the z direction.

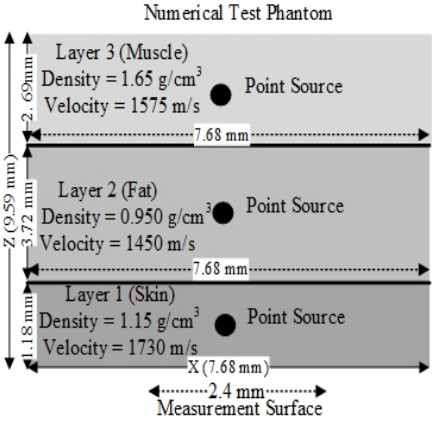

Figure 7.6: Numerical test fantom.

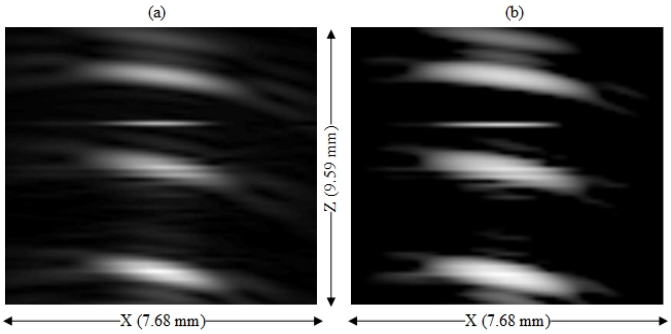

Figure 7.7: Numerical simulation results for the three-layered planar medium with the correct source locations using (5.82). (a) Source distribution in linear scale. (b) Source distribution in logarithmic scale (Dynamic range is 20 dB).

In Fig.7.6, we took three layered numerical test phantom. For the detection of the acoustic field, 32 point-like transducers with $\lambda_0/4$ an inter-element separation were placed at the bottom of the phantom ($f_0 = 5$ MHz, FBW = 100) for muscle, fat and skin. Transducer size is 2.4 mm. We performed the numerical simulations using Green's function for three layer medium. We obtained the explicit expression of Green's function by making similar calculations to the Chapter 6 and verified our inverse algorithm also for three-layer medium with the correct location of point source in all layers in Fig. 7.7.

Chapter 8

Conclusion

We derived analytical forward and inverse solution of the thermoacoustic wave equation in frequency domain for the planar multi-layer media with the sources existing in all layers by using continuity conditions on boundary surfaces, initial condition and radiation condition at infinity. As we were proving the forward and inverse solution for multi-layer media, we used method of Green's function. We performed numerical simulations for qualitative testing and comparison of the point-spread functions associated with the conventional solution and our layered inverse solution for $N = 1$, $N = 2$ and $N = 3$. We indicated the differences between the homogeneous and the layered solutions using numerical simulations and their results show that the conventional inverse solution based on a homogeneous medium assumption, as expected, produced incorrect locations of the point sources, whereas our inverse solution involving the multi-layer planar medium produces point sources at the correct locations. Performance of layered inverse is sensitive to the validity of the layer parameters and medium parameters used as prior information in the measured data. This means that the accurate estimation of the layer parameters is critically important for the effectiveness of the solution. Hence, computer simulation studies are conducted to investigate and then demonstrate the proposed solution. Our inverse solution based on multi-layer planar media applicable for a cross-sectional 2 dimensional imaging of the tissue structures such as breast, skin and abdominal where transducer size relatively smaller than the medium size.

References

[1] C. Guy, D. Ffytche, " An Introduction to The Principles of Medical Imaging," *Imperial College Press*, pp. 30-400, 2005.

[2] A.J., Angelsen, "Ultrasound Imaging," *Emantec AS*, pp. 130-200, 2000.

[3] W. Joines, R. Jirtle, M. Rafal, and D. Schaeffer, "Microwave power absorption differences between normal and malignant tissue," *Radiation Oncol. Biol. Phys.*, vol. 6, pp. 681-687, 1980.

[4] S. Chaudhary, R. Mishra, A. Swarup, and J. Thomas, "Dielectric properties of normal human breast tissues at radiowave and microwave frequencies," *Indian J. Biochem. Biophys.*, vol. 21, pp. 76-79, 1984.

[5] W. Joines, Y. Zhang, C. Li, and R. Jirtle, "The measured electrical properties of normal and malignant human tissues from 50-900 MHz," *Med. Phys.*, vol. 21, pp. 547-550, 1994.

[6] L. E. Larsen and J. H. Jacobi, "Medical Applications of Microwave Imaging," Piscataway, *NJ: IEEE Press*, 1986.

[7] S. Caorsi, A. Frattoni, G. L. Gragnani, E. Nortino, and M. Pastorino, "Numerical algorithm for dielectric-permittivity microwave imaging of inhomogeneous biological bodies," *Med. Biol. Eng. Comput.*, vol. NS-29, pp. 37-44, 1991.

[8] M. S. Hawley, A. Broquetas, L. Jofre, J. C. Bolomey, and G. Gaboriaud, "Microwave imaging of tissue blood content changes," *J. Biomed. Eng.*, vol. 13, pp. 197-202, 1991.

[9] P. M. Meaney, K. D. Paulsen, and J. T. Chang, "Near-field microwave imaging of biologically-based materials using a monopole transceiver system," *IEEE Trans. Microwave Theory Tech.*, vol. 46, pp. 31-45, 1998.

[10] R. A. Kruger, K. D. Miller, H. E. Reynolds, W. L. Kiser, D. R. Reinecke, and G. A. Kruger, "Breast cancer in vivo: contrast enhancement with thermoacoustic CT at 434 MHz-feasibility study," *Radiology*, vol.216, pp. 279-283, 2000.

[11] A. A. Oraevsky, A. A. Andreev, A. A. Karabutor, K. R. Declan Fleming, Z. Gatalica, H. Singh and R. O. Esenalier, "Laser optoacoustic imaging of the breast: detection of cancer angiogenesis," *Proc. SPIE* 3597, pp. 352-363, 1999.

[12] R. O. Esenaliev, A. A. Karabutov, F. K. Tittel, B. D. Fornage, S. L. Thomsen, C. Stelling and A. A. Oraevsky, "Laser optoacoustic imaging for breast cancer diagnostics: limit of detection and comparison with x-ray and ultrasound imaging," *Proc. SPIE* 2979, pp. 71-82, 1997.

[13] A. R. Kruger, L. Kiser William, K. D. Miller , H.E. Reynolds "Thermoacoustic CT: imaging principles," *Proc. SPIE 3916, Biomed. Optoacous.*, pp. 150-159, 2000.

[14] C. Gabriel, R. J. Sheppard, E. H. Grant, "The dielectric properties of biological tissues," *Physics in Medicine and Biology*, vol.41, pp. 2231-2249, 1996.

[15] P. Kuchment and L. Kunyansky, "Mathematics of thermoacoustic tomography: a survey in mathematics for industry," *E. J. Appl. Math.*, vol. 1, pp. 191-224, 2008.

[16] P. Beard, "Review: Biomedical photoacoustic imaging," *Interface Focus*, pp. 1-29, 2015.

[17] K. Maslov, L.V. Wang, D. K. Yao, C. Zang, "Photoacoustic measurement of the Grüneisen parameter tissue," *Journal of Biomedical Optics*, vol.19(1), pp. 1-6, 2014.

[18] M. Xu, and L. V. Wang, "Photoacoustic imaging in biomedicine," *Review of Scientific Instruments*, vol.77(4), pp. 041101-041122, 2006.

[19] V. E. Gusev and A. A. Karabutov, "Laser optoacoustics," *AIP*, USA, 1993.

[20] C. Li, and L. V. Wang, "Photoacoustic tomography and sensing in biomedicine," *Phys Med Biol.* vol. 54(19), pp. 59- 97, 2009.

[21] Y. Xu, D. Feng, and L. V. Wang, "Exact frequency-domain reconstruction for thermoacoustic tomography-I: Planar geometry," *IEEE Trans. Med. Imag.*, Vol. 21(7), pp. 823-828, JULY 2002.

[22] L.V. Wang and X. Yang , "Universal back-projection algorithm for photoacoustic computed tomography," *Physical Review E*, vol.71, pp. 016706(1-7), 2005.

[23] M. Idemen and A. Alkumru , "On an inverse source problem connected with photo-acoustic and thermo-acoustic tomographies," *Wave Motion*, vol. 49, pp. 595-604, 2012.

[24] R. W. Schoonover and M. Anastasio , "Image reconstruction in photoacoustic tomography involving layered acoustic media," *J. Opt. Soc. Am.*, vol. 28(6), pp. 1114-1120, 2011.

[25] M. Agranovsky and P. Kuchment, "Uniqueness of reconstruction and an inversion procedure for thermoacoustic and photoacoustic tomography with variable sound speed," *Inverse Problems*, vol. 23(5), pp. 2089-2102, 2007.

[26] Y. Hristova, P. Kuchment, and L. Nguyen, "Reconstruction and time reversal in thermoacoustic tomography in acoustically homogeneous and inhomogeneous media," *Inverse Problems*, vol. 24(5), pp. 055006, 2008.

[27] P. Stefanov and G. Uhlmann, "Thermoacoustic tomography with variable sound speed," *Inverse Problems*, vol. 25(7), pp. 075011, 2009.

[28] J. Qian, P. Stefanov, G. Uhlmann, and H. Zhao, "A new numerical algorithm for thermoacoustic and photoacoustic tomography with variable sound speed," *Dept. Comput. Appl. Math.*, Univ. California USA, pp. 10-81, 2010.

[29] B. T. Cox and B. E. Treeby, "Artifact trapping during time reversal photoacoustic imaging for acoustically heterogeneous media," *IEEE Trans. Med. Imag.*, vol. 29(2), pp. 387-396, 2010.

[30] M. Idemen, "Some universal properties of the Greens functions associated with the wave equation in bounded partially-homogeneous domains and their use in acoustic tomography," *Scientific Research Publishing*, pp. 483-499, 2017.

[31] L.V. Wang and H. Wu,"Biomedical Optics Principles and Imaging," *Wiley*, USA, pp. 285-316, 2007.

[32] E. L. Kinsler, A. R. Frey, A. B. Coppens and J. v. Sanders,3rd Ed.," Fundamentals Of Acoustics," *Wiley*, USA, pp. 98-121,1982.

[33] I. Stakgold and M. J. Holst, "Green's function and boundary value problems," *Wiley*, USA pp. 51-216, 2011.